

CAN WE PREDICT THE GLOBAL MAGNETIC TOPOLOGY OF A PRE-MAIN-SEQUENCE STAR FROM ITS POSITION IN THE HERTZSPRUNG–RUSSELL DIAGRAM?

S. G. GREGORY¹, J.-F. DONATI², J. MORIN^{3,4}, G. A. J. HUSSAIN⁵, N. J. MAYNE⁶, L. A. HILLENBRAND¹, AND M. JARDINE⁷

¹ California Institute of Technology, MC 249-17, Pasadena, CA 91125, USA; sgregory@caltech.edu

² IRAP-UMR 5277, CNRS & Université de Toulouse, 14 Av. E. Belin, F-31400 Toulouse, France

³ Institut für Astrophysik, Universität Göttingen, Friedrich-Hund-Platz 1, D-37077 Göttingen, Germany

⁴ Dublin Institute for Advanced Studies, School of Cosmic Physics, 31 Fitzwilliam Place, Dublin 2, Ireland

⁵ ESO, Karl-Schwarzschild-Str. 2, D-85748 Garching, Germany

⁶ School of Physics, University of Exeter, Exeter EX4 4QL, UK

⁷ School of Physics and Astronomy, University of St. Andrews, St. Andrews KY16 9SS, UK

Received 2012 January 30; accepted 2012 June 21; published 2012 August 1

ABSTRACT

Zeeman–Doppler imaging studies have shown that the magnetic fields of T Tauri stars can be significantly more complex than a simple dipole and can vary markedly between sources. We collect and summarize the magnetic field topology information obtained to date and present Hertzsprung–Russell (H-R) diagrams for the stars in the sample. Intriguingly, the large-scale field topology of a given pre-main-sequence (PMS) star is strongly dependent upon the stellar internal structure, with the strength of the dipole component of its multipolar magnetic field decaying rapidly with the development of a radiative core. Using the observational data as a basis, we argue that the general characteristics of the global magnetic field of a PMS star can be determined from its position in the H-R diagram. Moving from hotter and more luminous to cooler and less luminous stars across the PMS of the H-R diagram, we present evidence for four distinct magnetic topology regimes. Stars with large radiative cores, empirically estimated to be those with a core mass in excess of $\sim 40\%$ of the stellar mass, host highly complex and dominantly non-axisymmetric magnetic fields, while those with smaller radiative cores host axisymmetric fields with field modes of higher order than the dipole dominant (typically, but not always, the octupole). Fully convective stars above $\gtrsim 0.5 M_{\odot}$ appear to host dominantly axisymmetric fields with strong (kilo-Gauss) dipole components. Based on similarities between the magnetic properties of PMS stars and main-sequence M-dwarfs with similar internal structures, we speculate that a bistable dynamo process operates for lower mass stars ($\lesssim 0.5 M_{\odot}$ at an age of a few Myr) and that they will be found to host a variety of magnetic field topologies. If the magnetic topology trends across the H-R diagram are confirmed, they may provide a new method of constraining PMS stellar evolution models.

Key words: Hertzsprung–Russell and C–M diagrams – stars: evolution – stars: formation – stars: interiors – stars: magnetic field – stars: pre-main sequence

Online-only material: color figures

1. INTRODUCTION

At the end of the protostellar phase of spherical accretion, a newly formed and optically visible pre-main-sequence (PMS) T Tauri star is highly luminous due to its large surface area ($L_* \propto R_*^2$). The contracting star thus begins its journey toward the main sequence (MS) in the upper right of the $\log L_* - \log T_{\text{eff}}$ Hertzsprung–Russell (H-R) diagram while accreting material from its circumstellar disk. At this stage the temperature T and density ρ in the central regions of the star are not sufficient for thermonuclear reactions to occur, and the stellar luminosity is supplied by the release of the gravitational potential energy via the stellar contraction. During the fully convective phase of evolution the PMS star follows an almost vertical downward path in the H-R diagram, called the Hayashi track (Hayashi 1961).

As the gravitational contraction proceeds, the opacity κ in the central regions becomes dominated by free–free and bound–free transitions (e.g., Ward-Thompson & Whitworth 2011) for which $\kappa \propto \rho T^{-7/2}$. As the temperature continues to rise, the central opacity thus drops, the star becomes more transparent, and the radiative gradient decreases below the critical value required to support convection (see the discussion in Hartmann 2009) and a radiative core forms. This radiative core continues to grow reducing the depth of the convective

zone.⁸ Eventually the temperature and luminosity of the contracting star rise, and it leaves its Hayashi track and moves onto its Henyey track (Henyey et al. 1965), a process sometimes referred to as the “convective–radiative transition” (e.g., Mayne 2010). The rapid increase in effective temperature at a slowly increasing luminosity during the Henyey phase leads to a clear “gap” in color–magnitude diagrams of PMS clusters (Mayne et al. 2007). The size of the gap is dependent on the mass cut-off between fully and partially convective stars which itself is a function of stellar age, meaning that the gap can, in principle, be used as a distance-independent age indicator (Mayne & Naylor 2008).

Several observational results have been attributed to the development of a radiative core at the end of the fully convective phase of evolution. Rebull et al. (2006) argue that the ratio of X-ray to bolometric luminosity is systematically lower for stars with radiative cores compared to those on the fully convective

⁸ More massive T Tauri stars become entirely radiative during their PMS evolution and some develop convective cores on the main sequence if the power generated from thermonuclear reactions is sufficient (see, e.g., the models of Lejeune & Schaerer 2001). Stars with mass $\lesssim 0.35 M_{\odot}$ arrive on the main sequence and hydrogen fusion begins before a radiative core can develop, and thus retain a fully convective interior during their PMS evolution (Chabrier & Baraffe 1997).

portion of their mass tracks, with Mayne (2010) finding similar reductions in X-ray luminosities in older PMS clusters (the older the cluster the greater the fraction of stars that have ended the fully convective phase). Alexander & Preibisch (2012) invoke radiative core development to explain the reduction in the scatter in X-ray luminosities apparent in rotation–activity plots in older PMS star-forming regions. Furthermore, the growth of a radiative core appears to coincide with a reduction in the number of periodically variable T Tauri stars (Saunders et al. 2009). The authors attribute this result to differing cool spot distributions in fully and partially convective stars with large cool spots (where bundles of magnetic flux burst through the stellar surface into the atmosphere) on fully convective objects and smaller more numerous spots on stars with radiative cores which naturally lead to less rotationally modulated variability. All of these observational results can be qualitatively explained if the external magnetic field topology of T Tauri stars changes as the stellar internal structure transitions from fully to partially convective.

T Tauri stars have long been known to possess surface-averaged magnetic fields of order a kilo-Gauss as determined from Zeeman broadening measurements (e.g., Johns-Krull et al. 1999b; Johns-Krull 2007; Yang & Johns-Krull 2011 and references therein). Such strong magnetic fields can disrupt circumstellar disks at a distance of a few stellar radii (Königl 1991), provided that they are sufficiently globally ordered, a key requirement of magnetospheric accretion models (see Gregory et al. 2010 for a review). The disk truncation radius R_t is set by the interplay between the strength of the stellar magnetosphere at the inner disk, which can be approximated from the polar strength of the dipole component of the multipolar stellar magnetic field at the surface of the star B_{dip} , and the disk mass accretion rate \dot{M} . Larger disk truncation radii are expected for stronger dipole components and/or weaker mass accretion rates as $R_t \propto B_{\text{dip}}^{4/7} \dot{M}^{-2/7}$ (e.g., Königl 1991), quantities which may vary significantly with time. Typical disk truncation radii are believed to be $\sim 5 R_*$ (Gullbring et al. 1998), or ~ 0.05 AU for a prototypical $2 R_\odot$ T Tauri star. Such small scales, within or comparable to typical dust sublimation radii, can be probed with high-resolution spectroscopy of gas emission lines (e.g., Najita et al. 2003) and by long baseline interferometry (see Millan-Gabet et al. 2007; Akeson 2008 and Millan-Gabet et al. 2007 for reviews of the technique). Gas is typically found to extend closer toward the star than the dusty component of the disk for both T Tauri stars and the related more massive Herbig Ae/Be stars (Kraus et al. 2008; Isella et al. 2008; Eisner et al. 2009, 2010; Ragland et al. 2009). For some sources the gas component of the disk provides a significant amount of the detected inner disk flux (Akeson et al. 2005). The inner disk gas couples to the field lines of the stellar magnetosphere and is channeled onto the stellar surface at high velocity, where it shocks and produces detectable hot spots that are the source of continuum emission in excess of the stellar photospheric emission, as well as soft X-rays (e.g., Calvet & Gullbring 1998; Kastner et al. 2002; Argiroffi et al. 2011, 2012). The geometry and distribution of accretion hot spots is a strong function of the stellar magnetospheric geometry (Romanova et al. 2004a; Gregory et al. 2005, 2006; Mohanty & Shu 2008).

Complementing the Zeeman broadening analysis, which is carried out in unpolarized light, measurement of the level of circular polarization in both accretion-related emission lines and photospheric absorption lines allows information to be derived about the field topology itself (Valenti & Johns-Krull 2004;

Donati et al. 2007, 2008a, 2010b). The large-scale magnetic fields of accreting T Tauri stars appear to be well ordered, and are simpler than the complex and loopy surface field regions (e.g., Valenti & Johns-Krull 2004). However, although the large-scale field that is interacting with the inner disk is somewhat dipole-like in appearance, the path of field lines close to the star, and consequently the magnetospheric accretion flow, is distorted close to the stellar surface by the complex field regions (Gregory et al. 2008; Adams & Gregory 2012).

Magnetic surface maps have now been published for a number of accreting T Tauri stars (Donati et al. 2007, 2008a, 2010a, 2010b, 2011a, 2011b, 2011c, 2012; Hussain et al. 2009; Skelly et al. 2012), one non-accreting weak-line T Tauri star (Skelly et al. 2010), and a few older post T Tauri stars (Dunstone et al. 2008a; Marsden et al. 2011; Waite et al. 2011), derived from the technique of Zeeman–Doppler imaging (ZDI), as we discuss in the following section. Most of the published magnetic maps have been obtained as part of the Magnetic Protostars and Planets (MaPP) project. The main goal of this large program with the ESPaDOnS spectropolarimeter at the Canada–France–Hawai‘i telescope (Donati 2003), and the twin instrument NARVAL at the T el escope Bernard Lyot in the Pyren ees (Auri ere 2003), is to investigate variations in the magnetic topology of accreting T Tauri stars of different mass,⁹ age, accretion rate, rotation period, and outflow properties (see Donati et al. 2010b for a brief introduction to the program).

The initial MaPP results have demonstrated that accreting T Tauri stars possess multipolar magnetic fields but with dipole components that are strong enough to disrupt the inner disk at distances of up to several stellar radii. Intriguingly, the field complexity and the polar strength of the dipole component appear to increase and decrease respectively when comparing stars with fully convective interiors to those which have developed radiative cores (e.g., Donati et al. 2011b)—a concept that we explore fully in this paper. Similar variations in magnetic field topology of MS M-dwarfs that span the fully convective divide have been discovered by Morin et al. (2008, 2010) and Donati et al. (2008b).

On the MS stars below $\sim 0.35 M_\odot$, later than roughly spectral type M4, have a fully convective internal structure while more massive stars do not (Chabrier & Baraffe 1997). Fully convective M-dwarfs close to the fully convective limit ($\gtrsim 0.2 M_\odot$) host simple, axisymmetric magnetic fields with strong dipole components (Morin et al. 2008). M-dwarfs of earlier spectral type which are partially convective with small radiative cores have magnetic fields with weaker dipole components that are dominantly axisymmetric (most of the magnetic energy is in the poloidal field modes; Donati et al. 2008b). M-dwarfs with more substantial radiative cores have both weak dipole components and more complex magnetic fields (less magnetic energy in the poloidal field modes; Donati et al. 2008b). This behavior is illustrated in Figures 1 and 2. Clear differences in (the large scale) stellar magnetic field topologies are observed as a direct manifestation of the differing stellar internal structure and therefore, presumably, the different type of dynamo mechanism operating in fully and partially convective stars. Stars with outer convective zones and radiative cores are believed to possess a solar-like tachocline, a shear layer between the core and envelope, whereas fully convective stars lack this interface, and the dynamo process is different (e.g., Browning 2008).

⁹ In this paper we refer to stars of mass $M_* \lesssim 0.5 M_\odot$ as low mass, $0.5 \lesssim M_*/M_\odot \lesssim 1.0$ as intermediate mass, and $M_* \gtrsim 1.0 M_\odot$ as high-mass PMS stars.

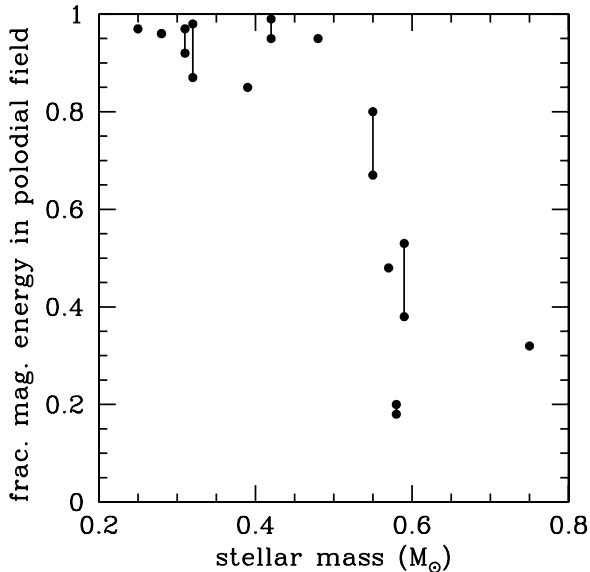


Figure 1. Magnetic energy in the poloidal field modes relative to the magnetic energy in all field modes, as a function of the mass of main-sequence M-dwarfs, determined via a spherical harmonic decomposition of the magnetic maps derived from ZDI studies (data presented in Morin et al. 2008 and Donati et al. 2008b). Points joined by vertical bars represent stars observed at two different epochs. For stars with small radiative cores (those above $\sim 0.35 M_{\odot}$; Chabrier & Baraffe 1997), the field remains dominantly poloidal until $\sim 0.5 M_{\odot}$. For more massive stars with large radiative cores, strong toroidal field components develop with increasing stellar mass and the fractional magnetic energy in the poloidal field decreases. This increase in field complexity with the size of a radiative core results in the dipole component of the field becoming less significant relative to the higher order field components. Completely convective stars have simpler, mostly poloidal, large-scale fields, although very low mass fully convective M-dwarfs (below $\sim 0.2 M_{\odot}$) are also capable of hosting complex magnetic fields (see Morin et al. 2010; data points not shown here).

Morin et al. (2011), following on from Goudard & Dormy (2008), point out that the simple large-scale fields of many fully convective M-dwarfs are more akin to the simple magnetic topologies of the gas giant planets within our solar system (e.g., Willis & Osborne 1982), rather than the messy and complex fields observed on active zero-age MS K-type stars (e.g., Donati et al. 2003). However, the lowest mass M-dwarfs ($\lesssim 0.2 M_{\odot}$) with very similar stellar parameters (rotation rate and mass) can show drastically different magnetic field topologies (Morin et al. 2010). This may be caused by a bistable dynamo process, with a weak and a strong field dynamo branch, such that the two different dynamo regimes co-exist over a certain range of parameters (see Figure 4 of Morin et al. 2011, adapted from Roberts 1988). Fully convective stars in the strong field regime maintain steady and simple axisymmetric dominantly dipolar magnetic fields while fully convective stars with identical stellar parameters but in the weak field regime host complex multipolar fields which evolve rapidly in time and have weak dipole components.

In this paper we explore the trends in the magnetic field topology of PMS stars with stellar internal structure that are now emerging from spectropolarimetric observing programs. Unlike MS M-dwarfs, however, the internal structure of PMS stars is changing rapidly due to the stellar contraction and (if the star is massive enough) the development of a radiative core. The stellar age is thus an important parameter in addition to mass when examining magnetic field topology variations for PMS stars caused by changes in the internal structure of the star.

Given the importance of the magnetic field topology in controlling the star–disk interaction, in Section 2 we summarize

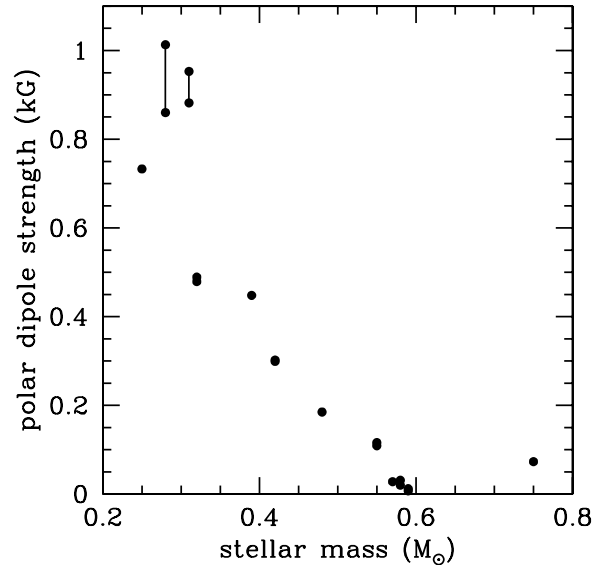


Figure 2. Decay of the polar strength of the $m = 0, \ell = 1$ dipole component B_{dip} for the main-sequence M-dwarf stars observed by Morin et al. (2008) and Donati et al. (2008b). Points connected by vertical bars represent stars observed at two different epochs. Low-mass completely convective stars have strong dipole components. As the stellar mass, and therefore the size (volume) and mass of the radiative core, increases above the limit for full convection the strength of the dipole component decays rapidly.

the magnetic topology information, and the fundamental stellar parameters, that have been obtained to date for accreting PMS stars. In Section 3, we position the stars with derived magnetic maps onto H-R diagrams constructed from two different PMS evolutionary models, examine the role of the development of a radiative core in setting the magnetic field topology, and compare the field topologies of PMS stars to those of MS M-dwarfs with similar internal structures. In Section 4, we argue that it may be possible to predict the global magnetic topology characteristics of a given star (e.g., whether or not the field will have a strong dipole component is dominantly axisymmetric or non-axisymmetric, etc.) based on its position in the H-R diagram. Our ability to do this, however, is dependent on a number of caveats and assumptions including the accuracy with which the star can be positioned in the H-R diagram observationally and the veracity of the PMS evolutionary models themselves. In Section 5 we explore the implications of magnetic topology variations in terms of the star–disk interaction, while Section 6 contains our conclusions.

2. T TAURI MAGNETIC FIELD TOPOLOGY

Over the past few years spectropolarimetric ZDI studies have revealed that the field topology of T Tauri stars can vary significantly between sources (Donati 2001 and Donati & Landstreet 2009 provide reviews of the basic methodology of ZDI, while details specific to accreting T Tauri stars are discussed in Donati et al. 2010b and Hussain 2012). Magnetic maps of T Tauri stars are constructed by measuring the circular polarization (Stokes V) signal in both accretion-related emission lines and in photospheric absorption lines, over at least one complete stellar rotation cycle and in practice several cycles. Circular polarization can be measured directly in the accretion-related emission lines, for example, He I 5876 Å (Johns-Krull et al. 1999a; Donati et al. 2008a) or the Ca II infrared triplet (Donati et al. 2007), but the signal is often too weak in a given individual magnetically sensitive photospheric absorption

line. In practice, cross-correlation techniques, such as least-squares deconvolution, are employed in order to extract information from as many lines as possible. The signal-to-noise ratio (S/N) of the resulting average Zeeman signature is several tens of times larger than that of a single spectral line (Donati et al. 1997). Magnetic surface features produce distortions in the Stokes V signal that depend on the latitude and longitude of the magnetic region and on the orientation of the field lines. By monitoring how such distortions move through the Stokes V profile due to the stellar rotation the two-dimensional distribution of magnetic polarities across the surface of stars can be determined using maximum entropy reconstruction techniques (Brown et al. 1991), as well as the field orientation within the magnetic regions (Donati & Brown 1997).

The ability to derive maps of the surface magnetic topology of T Tauri stars (and of stars generally) is subject to some limitations, as discussed in detail by Hussain (2012). ZDI, like all polarization techniques, suffers from the effects of flux cancellation. Photons received from regions of the stellar atmosphere permeated by opposite polarity magnetic fields are polarized in the opposite sense. Their signals can therefore cancel, resulting in a net polarization signal of zero. Due to this flux cancellation effect it is possible to recover information only about the medium-to-large-scale field topology. Detailed features on scales that can be resolved in solar magnetograms remain below the resolution limit achievable in stellar magnetic maps (see Gregory et al. 2010 for further discussion). Spectropolarimetric Stokes V studies thus likely miss a large fraction of the total magnetic flux (Reiners & Basri 2009), presumably contained within the tangled and complex small-scale field, perhaps on the scale of bipolar groups detected on the Sun. The resolution achievable in stellar magnetic maps is also dependent on the stellar rotation period and the inclination.

Once magnetic maps have been derived, the field topology can be reconstructed as the values of the coefficients of a spherical harmonic decomposition and the strength of the various field modes determined (e.g., Donati et al. 2006). For example, it is possible to decompose the field into the sum of a poloidal plus a toroidal component, and to calculate the strength, tilt, and phase of tilt, of the various multipole moments (Donati et al. 2010b). Due to the stellar inclination surface magnetic field information cannot be obtained across portions of the stellar surface that remain hidden from view to an observer. This limitation is important when constructing three-dimensional models of T Tauri magnetospheres via field extrapolation from the magnetic maps (e.g., Gregory et al. 2008) as an assumption must be made whether to favor the symmetric (the odd ℓ number modes, e.g., the dipole, the octupole, the dotriacontapole, etc.) or antisymmetric (the even ℓ number modes, e.g., the quadrupole, the hexadecapole, etc.) field modes. As part of the tomographic imaging process maps of the surface distribution of cool (dark) spots and accretion-related hot spots are also derived (Donati et al. 2010b). These maps suggest that for the bulk of accreting T Tauri stars gas in accretion columns impacts the stellar surface at high latitudes close to the poles. This suggests that it is antisymmetric field modes, like the dipole and the octupole, that dominate. If the symmetric field modes were to dominate then the majority of the gas would accrete onto the equatorial regions, for example, Long et al. (2007), which is not observed. The choice of whether to favor the symmetric or anti-symmetric modes, although important when constructing three-dimensional models of the stellar magnetosphere, does

not fundamentally change the appearance of the magnetic field maps (Hussain 2012).

Magnetic maps have now been published for a number of T Tauri stars (see Gregory & Donati 2011 for a review). Some T Tauri stars host simple axisymmetric large-scale magnetic fields that are dominantly dipolar (AA Tau and BP Tau) or where a higher order field mode dominates (typically, but not always, the octupole; V2129 Oph, GQ Lup, TW Hya, and MT Ori), while others host highly complex magnetic fields that are dominantly non-axisymmetric with many high-order multipole components (V4046 Sgr AB, CR Cha, CV Cha, and V2247 Oph). In Appendix A, we provide detailed information about the magnetic field topology of every accreting T Tauri star for which magnetic maps have been derived to date, with the main stellar properties listed in Tables 1 and 2. The stellar internal structure information, masses, and ages have been derived by placing the stars onto the H-R diagram as discussed in Section 3.1.

The effective temperatures T_{eff} and luminosities L_* listed in Table 1 are the values that were adopted in each of the papers where the magnetic maps were published, as listed in the reference column of the table, and to which readers are referred for detailed discussion. The one exception is the luminosity of V2247 Oph which we have updated using a more refined estimate of the distance to the ρ -Oph star-forming region (see Appendix A.3.4). Typically the effective temperatures were sourced from previously published literature values as derived from high-resolution spectra. The exception to this is GQ Lup for which Donati et al. (2012) derived a new T_{eff} as previous literature values were estimated from low-resolution spectra and proved to be highly discrepant. As a consistency check, a new spectral classification tool (called MagIcS) has been developed and applied to the ESPaDOnS spectra and has been tested for a number of MS and PMS template stars (J.-F. Donati, in preparation). The assumed errors in T_{eff} values are also taken from the previously published values, or assumed to be 100 K when no error estimate is available (errors from the spectral classification tool are <100 K).

Luminosities were derived from the visual magnitudes and distance estimates to the various star-forming regions, taking account of the uncertainty associated with the presence of surface cool spots. In the papers with published magnetic maps the error in $\log(L_*/L_\odot)$ is typically assumed to be 0.1 dex, with the exception of CR Cha, CV Cha, and MT Ori. Further stellar parameters, including the stellar rotation periods adopted during the magnetic map reconstruction process, are listed in Table 2. Given the importance of the dipole component in controlling the star-disk interaction, see Section 5.1, we also list the polar strength of the dipole component of the multipolar magnetic field of each star.

In Table 1, we also highlight which stars in our sample are part of binary systems and the binary separation. For those with large separations the presence of a companion star is not expected to have any influence on the stellar magnetic field topology. Those with the smallest separations, V2247 Oph and V4046 Sgr AB, are found to host complex non-axisymmetric magnetic fields (Donati et al. 2010a, 2011c). We find little difference when comparing the field complexity found on single and binary stars. For example, both components of HD 155555 (Dunstone et al. 2008a), a tidally locked close post T Tauri binary, have magnetic field topologies and surface differential rotation measurements that are consistent with those of single stars with similar spectral types (Dunstone et al. 2008b). Similar results have also been

found for the M-dwarf eclipsing binary YY Gem (J. Morin et al., in preparation). Therefore, we do not expect that binarity plays a significant role in setting the field complexity, although it clearly plays a role in the evolution of the large-scale coronal field due to the interaction between the stellar magnetospheres if the binary separation is sufficiently small, e.g., DQ Tau (Salter et al. 2010; Getman et al. 2011). Such large-scale changes in the coronal field that triggers flares appear to be generated by only small changes in the surface field topology, as determined by contemporaneous spectropolarimetric and X-ray observations (Hussain et al. 2007).

3. INFORMATION FROM THE HERTZSPRUNG–RUSSELL DIAGRAM

In this section we construct H-R diagrams using the stars listed in Table 1 and contrast mass, age, and internal structure properties derived from two different PMS evolutionary models. We discuss the variation in the magnetic field topology of stars across the diagram and explore the similarities between the field topologies of PMS stars and MS M-dwarfs with similar internal structures.

3.1. Magnetic Field Topology and Stellar Internal Structure

Figure 3 shows H-R diagrams constructed from the Siess et al. (2000) and the Pisa (Tognelli et al. 2011) PMS stellar evolution models. The mass tracks are colored according to the internal structure of the star—black for fully convective stars and red for partially convective stars with radiative cores. The H-R diagrams also include internal structure contours, the solid blue lines that connect stars of different effective temperature and luminosity, equivalently mass and age, but with the same internal structure (the same values of M_{core}/M_*). The solid blue line on the right is the fully convective limit. Stars that lie in the region of the H-R diagram above and to the right of the fully convective limit have fully convective interiors, and those in the region below and to the left have radiative cores, or are entirely radiative for the more massive stars beyond a certain age.

The points in Figure 3 are the stars listed in Table 1 and Appendix A with different symbols representing stars with different large-scale magnetic field topologies, as detailed in the caption. The stellar masses, ages, and radiative core masses derived from the Siess et al. (2000) and the Pisa (Tognelli et al. 2011) models are listed in Table 2. Generally, the masses derived from both models agree to within $\sim 10\%$, at least for the small sample of stars considered in this work. The exceptions are V2129 Oph and MT Ori which have masses $\sim 20\%$ and $\sim 40\%$ larger respectively in the Siess et al. (2000) models. With the exception of the lowest mass star V2247 Oph, the isochronal ages are consistently younger in the Tognelli et al. (2011) models. The largest age differences occur for high-mass T Tauri stars, as well as for TW Hya.

It can be seen from Figure 3 that more massive PMS stars leave their Hayashi tracks at a younger age and their radiative cores grow more rapidly than those of lower mass stars (see Appendix B for further details). There is no general trend in the core mass relative to the stellar mass (M_{core}/M_*) between the models; some stars have larger cores in one model, but in the same model other stars have smaller cores. Nevertheless it is encouraging that, with the exception of MT Ori, if a given star has ended the fully convective phase in one model, it has also done so in the other model. In this paper we choose to consider variations in the stellar internal structure by considering the

fractional radiative core mass M_{core}/M_* rather than considering the variation in the fractional radiative core radius R_{core}/R_* . This is because once a core develops, a change in the ratio M_{core}/M_* is a direct reflection of the growth of the radiative core, assuming that in the T Tauri phase the star is no longer accumulating significant mass via spherical infall and the stellar mass is set. In contrast, changes in the ratio R_{core}/R_* represents both the growth of the core and the radius decrease of the contracting PMS star, see Appendix B. The mass of the radiative core is therefore our preferred internal structure proxy, although it is directly related to the core radius as $M_{\text{core}} \propto R_{\text{core}}^3$ for a polytropic star. Once a star evolves onto the MS and its internal structure and radius have settled, both internal structure proxies can be used.

3.2. Intermediate- and High-mass T Tauri Stars ($\gtrsim 0.5 M_{\odot}$)

It appears that the general characteristics of the large-scale magnetic topology of an accreting T Tauri star ($\gtrsim 0.5 M_{\odot}$) are strongly related to the star’s position in the H-R diagram (see Figure 3). Stars which have similar internal structures (but very different mass/age and effective temperature/luminosity) appear to have similar magnetic field topologies: (1) stars in the completely convective regime (at least those above $\sim 0.5 M_{\odot}$ at an age of \sim few Myr; see Section 3.3 where we discuss low-mass T Tauri stars) have strong dipole components to their magnetic fields and their fields are dominantly axisymmetric (AA Tau and BP Tau); (2) stars with small radiative cores and large outer convective zones have magnetic fields that are dominantly axisymmetric and have high-order components that dominate the dipole (V2129 Oph, GQ Lup, TW Hya, and MT Ori—at least in the Siess et al. (2000) model for the latter, see below); and (3) more evolved stars with substantial radiative cores and small outer convective zones have complex non-axisymmetric magnetic fields with weak dipole components (V4046 Sgr AB, CR Cha and CV Cha). In general, the larger the radiative core the more complex the large-scale magnetic field, and the weaker the dipole component (see Table 2).

We note that the magnetic field of MT Ori is largely axisymmetric and the octupole, the dotriacontrapole, and the $\ell = 7$ field mode dominate the dipole. Its magnetic field is more similar to those of V2129 Oph, TW Hya, and GQ Lup, all of which have small radiative cores, and very different to those of the fully convective stars AA Tau and BP Tau. It thus seems likely that MT Ori has developed a radiative core, and the Siess et al. (2000) models give a more accurate representation of the stellar structure in this region of the H-R diagram (the Tognelli et al. 2011 models suggest that MT Ori is still fully convective). This argument is further supported by the observed trends in the field topology with varying internal structure for MS M-dwarfs on either side of the fully convective divide, as we discuss in Section 3.4.

3.3. Low-mass T Tauri Stars ($\lesssim 0.5 M_{\odot}$)—Dynamo Bistability?

The low-mass T Tauri regime ($\lesssim 0.5 M_{\odot}$) is, with the exception of V2247 Oph, an unexplored region of the H-R diagram in terms of stellar magnetic field topologies. Intriguingly, the field topology of V2247 Oph is complex and non-axisymmetric with a weak dipole component and resembles the fields of more massive T Tauri stars with substantial radiative cores rather than that of the more massive fully convective stars. We therefore speculate that a bistable dynamo process with weak and strong field branches operates among the lowest mass fully convective PMS stars, similar to the lowest mass MS M-dwarfs discussed at

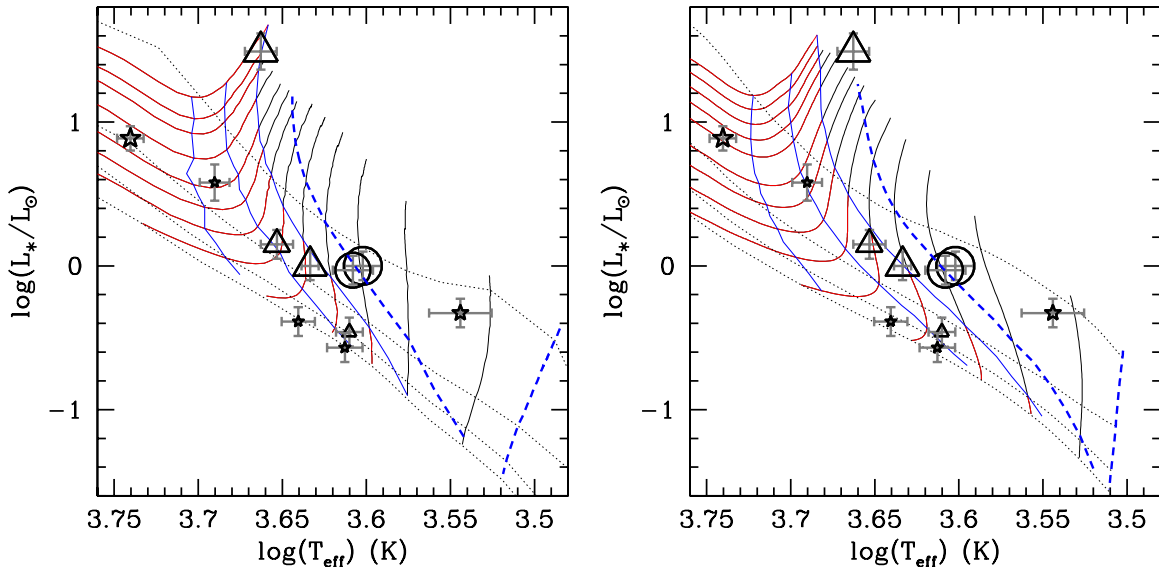


Figure 3. H-R diagrams constructed from the Siess et al. (2000) PMS evolution models (left) and the Pisa models (right; Tognelli et al. 2011). The mass tracks (solid black/red lines) from right to left represent $M_* = 0.3 M_\odot$ to $1.9 M_\odot$ in steps of $0.2 M_\odot$, then 2.2, 2.5, 2.7, $3.0 M_\odot$ for the Siess et al. (2000) diagram, and 2.2, 2.4, 2.6, 2.8, $3.0 M_\odot$ for the Tognelli et al. (2011) diagram (due to the differing grid resolutions of the models). Black (red) segments represent stars with fully convective interiors (those which have developed radiative cores). The solid blue lines are internal structure contours, with the right-hand line the fully convective limit, the middle (left-hand) line is the loci of stars with core masses of $M_{\text{core}}/M_* = 0.4$ (0.8). Isochrones (dotted lines) are shown for ages of 1, 5, 10, and 15 Myr from the upper right to the lower left. The black symbols are stars with published magnetic maps (see Table 2), circles are stars with dominant dipole components and axisymmetric fields, triangles are stars with dominant high-order field components ($\ell > 1$) and axisymmetric magnetic fields, and asterisks are stars with complex non-axisymmetric magnetic fields with weak dipole components. The size of the symbol is proportional to the stellar rotation period. Stars which have spent longer with radiative cores (weaker dipole components) are typically faster rotators than fully convective stars (with strong dipole components) in the intermediate- and high-mass regimes ($\gtrsim 0.5 M_\odot$). The dashed blue lines are upper and lower limits on a boundary separating two different magnetic topology regimes within the fully convective region of the H-R diagram; see Section 3.3.

(A color version of this figure is available in the online journal.)

the end of Section 1 (see Morin et al. 2011, their Figure 4 in particular). V2247 Oph would then belong to the weak field branch, while another fully convective star with similar stellar parameters but which belonged to the strong field dynamo branch would host a simple magnetic field with a strong dipole component. Once the low-mass T Tauri regime has been explored in detail we expect that stars with a variety of field topologies will be found, some with weak dipole components corresponding to the weak field dynamo branch and some with strong dipole components corresponding to the strong field dynamo branch.

As magnetic maps have yet to be obtained for the lowest mass fully convective PMS stars, the exact boundary between the strong dipole component regime and the bistable dynamo regime across the H-R diagram is unconstrained observationally, and also theoretically. As bistable dynamo behavior for MS M-dwarfs only occurs for stellar masses $\lesssim 0.2 M_\odot$, it is tempting to use this as the boundary separating the regions of fully convective PMS stars with strong dipole components (those with $M_* \gtrsim 0.2 M_\odot$) and those fully convective stars where some host fields with strong dipole components while other stars with similar parameters host complex fields with weak dipole components (those with $M_* \lesssim 0.2 M_\odot$).¹⁰ The $0.2 M_\odot$ boundary is illustrated as the right-hand dashed blue line in the H-R diagrams in Figure 3. However, for MS M-dwarfs whose internal structure and therefore presumably the dynamo magnetic field generation process has settled, the $0.2 M_\odot$ boundary is $\sim 60\%$

of the MS fully convective limit of $\sim 0.35 M_\odot$. PMS stars are still contracting, however, and as the boundary between stars which are fully convective and those which are not is a function of age (see Appendix B), we can also speculate that the mass boundary below which bistable dynamo behavior occurs is itself a function of age. The left-hand dashed blue line in Figure 3 illustrates this alternative boundary which occurs at a stellar mass that is 60% of the fully convective limit at that age. Thus, for a given bistable dynamo boundary, fully convective stars to the left of the boundary in the H-R diagram would have simple axisymmetric fields with strong dipole components; stars to the right would be in the bistable regime and may host a variety of field topologies just like the latest spectral-type (lowest mass) M-dwarfs. Taking the age-dependent boundary defined in Figure 3 would mean that both AA Tau and BP Tau are actually in the bistable dynamo regime, and with simple magnetic fields with strong dipole components they would be on the strong field dynamo branch. In reality, the two dashed blue lines in Figure 3 likely represent upper and lower limits to the true bistable dynamo limit. Clearly more data, and in particular more ZDI studies, are required for fully convective T Tauri stars to better constrain this limit and test our predictions.

3.4. Comparison with the Magnetic Topologies of MS M-dwarfs

Although the links between T Tauri magnetic field topologies and stellar internal structure discussed in Sections 3.2 and 3.3 are thus far based on a limited sample of PMS stars, similar trends have been found for MS M-dwarfs on either side of the fully convective divide (Donati et al. 2008b; Morin et al.

¹⁰ Recently Schrunner et al. (2012) have published a series of numerical simulations that suggest that bistable dynamo behavior can occur for all MS M-dwarfs in the fully convective regime, including those close to the fully convective limit. Presently there is no observational evidence for this, with bistable behavior only apparent for stars (both MS and PMS) located well below the fully convective limit.

2008, 2010). For MS M-dwarfs the transition from dominantly axisymmetric to non-axisymmetric fields occurs once the stellar mass exceeds $\sim 0.5 M_{\odot}$ (see Figure 1) which corresponds roughly to $M_{\text{core}}/M_{*} \approx 0.4$ (the Siess et al. 2000 models give $M_{\text{core}}/M_{*} = 0.26$ for M-dwarfs of Siess mass $0.5 M_{\odot}$ and 0.44 for $0.6 M_{\odot}$).

The trends in magnetic topology of MS M-dwarfs across the fully convective limit thus roughly match those found from ZDI studies of PMS stars with similar internal structures, although there may be one subtle difference. T Tauri stars with small radiative cores ($0 < M_{\text{core}}/M_{*} \lesssim 0.4$) host axisymmetric magnetic fields but field modes of higher order than the dipole dominate (typically, but not always, the octupole, e.g., TW Hya, V2129 Oph, and GQ Lup). In contrast, M-dwarfs with similar fractional radiative core mass (M_{core}/M_{*}) host axisymmetric fields but the dipole component (although similarly weaker than that of fully convective stars) is the dominant field mode. These M-dwarfs have small inclinations, closer to pole-on. In such cases it is difficult to recover field topology information at low stellar latitudes, and to reliably infer field modes above the dipole when the dipole component is strong (large polar cool spots, e.g., that on TW Hya, help alleviate this problem in PMS stars with similarly low inclinations). This apparent difference between the PMS and MS sample may just be observational bias.

Alternatively, if the difference between the samples is real, it may be due to the rapidly changing internal structure of a PMS star with the core continuing to grow as the star evolves toward the MS. The growth rate of the core (the rate of increase of the ratio M_{core}/M_{*}) is more rapid the higher the stellar mass (see Appendix B). Thus, as higher mass stars transition from fully convective to partially convective, the dipole component of their magnetic fields may decay more rapidly the faster the core develops. Taking V2129 Oph and TW Hya as examples, although both currently have small radiative cores similar in size to mid-spectral-type M-dwarfs ($\sim M4-M5$ or $0.35-0.5 M_{\odot}$) of $\sim 20\%$ of their stellar mass, by the time they arrive on the MS they will have substantial radiative cores with $M_{\text{core}}/M_{*} \approx 0.95$ and ≈ 0.75 , respectively, and be of spectral type $\sim F7$ and $\sim K3$ (Siess et al. 2000). Although TW Hya and V2129 Oph currently have internal structures that are comparable to mid M-dwarfs, they will differ substantially by the time they arrive on the MS. By this stage their field topologies will likely resemble the more complex fields found for stars with small outer convection zones, like CR Cha, CV Cha, and V4046 Sgr AB, and the earlier spectral-type M-dwarfs. In other words, we are observing the PMS stars at a stage of their evolution where their large-scale magnetic fields are in the process of transitioning from simple to more complex fields. This may explain the one subtle difference between PMS magnetic field topologies and those of MS M-dwarfs with currently similar internal structures.

4. CAN WE PREDICT THE MAGNETIC FIELD TOPOLOGY OF T TAURI STARS?

4.1. The Magnetic Hertzsprung–Russell Diagram

As summarized above, ZDI studies have revealed that T Tauri stars host multipolar magnetic fields; however, the field topology seems to be strongly linked to the stellar internal structure, and consequently to how the magnetic field is generated and maintained by differing dynamo mechanisms. Empirically, we define four distinct magnetic topology regions across the PMS, see Figure 4, defined as we move from upper left

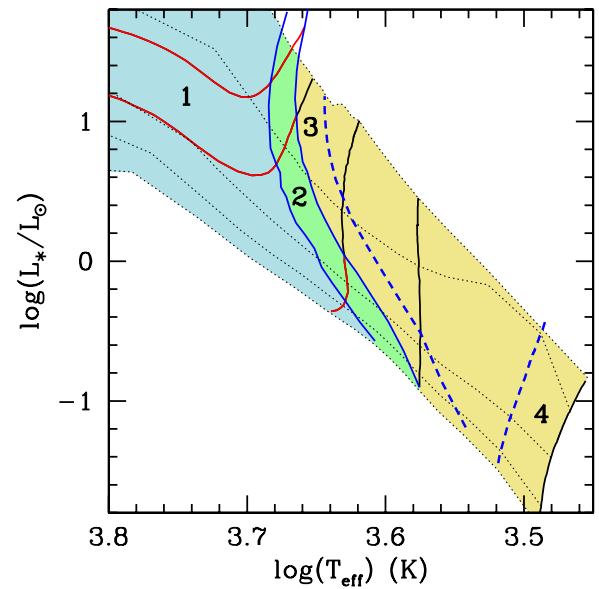


Figure 4. H-R diagram constructed from the models of Siess et al. (2000) assuming $Z = 0.02$ with convective overshooting. The mass tracks, for $M_{*} = 0.1, 0.5, 1.0, 2.0,$ and $3.0 M_{\odot}$, are black in the fully convective phase and red in the radiative core phase. The isochrones (dotted lines) are for ages of 0.25, 1, 5, 10, and 15 Myr. The solid blue lines connect stars in the H-R diagram with the same internal structure; on the right, it represents the fully convective limit, and on the left stars with $M_{\text{core}}/M_{*} = 0.4$. ZDI studies of T Tauri stars, and the comparable magnetic trends measured for main-sequence M-dwarfs with similar stellar internal structure, suggest that the general magnetic topology characteristics of stars vary across the different colored regions. In the blue region (region 1—stars with substantial radiative cores; $M_{\text{core}}/M_{*} \gtrsim 0.4$) stars have complex fields and weak dipole components. In the green region (region 2—stars with small radiative cores; $0 < M_{\text{core}}/M_{*} \lesssim 0.4$) stars have magnetic fields that are largely axisymmetric with dominant high-order field components ($\ell > 1$). In the yellow region stars are fully convective. Stars close to the fully convective limit (region 3) have strong dipole components to their multipolar magnetic fields. Below some boundary within the fully convective regime we expect bistable dynamo behavior and that we will find a mixture of stars, some with simple axisymmetric fields with strong dipole components and some with complex non-axisymmetric fields with weak dipole components. The dashed blue lines, defined in Section 3.3, denote possible upper and lower limits between this, region 4, and region 3. We stress that the region boundaries are empirical and are poorly constrained observationally and theoretically (see Section 4.2). More data are required to confirm the exact boundaries which may also vary with stellar mass.

(A color version of this figure is available in the online journal.)

(warm/luminous) to lower right (cool/faint) in the $\log L_{*}$ – $\log T_{\text{eff}}$ H-R diagram.

1. Region 1 (blue in Figure 4): stars with substantial radiative cores $M_{\text{core}}/M_{*} \gtrsim 0.4$. In this region stars have complex magnetic fields with many high-order components. The fields are highly non-axisymmetric and the dipole component is weak. This region contains the most massive T Tauri stars, typically those of spectral type G or early K, and also older stars of later spectral type. V4046 Sgr AB, CR Cha, and CV Cha lie in this region.
2. Region 2 (green in Figure 4): stars with small radiative cores $0 < M_{\text{core}}/M_{*} \lesssim 0.4$. In this region stars have magnetic fields that are dominated by strong high-order field components. The dipole component may be weak or strong but it contains less magnetic energy than the higher order field modes. The fields are largely axisymmetric. MT Ori, TW Hya, V2129 Oph, and GQ Lup lie in this region.
3. Region 3 (yellow in Figure 4): fully convective stars to the left of some boundary between the dashed blue lines. In this

region stellar magnetic fields are axisymmetric with strong (kilo-Gauss) dipole components. AA Tau and BP Tau likely lie in this region.

4. Region 4 (within the yellow region in Figure 4): fully convective stars to the right of some boundary between the dashed blue lines. The boundary between this region and region 3 is not well defined observationally. The dashed blue lines in Figure 4 are possible upper and lower limits to the true boundary (see Section 3.3). By comparison to the magnetic topologies of the lowest mass fully convective M-dwarfs we expect that this region will be populated by stars with a mix of magnetic topologies, the dynamo process being bistable with a strong and a weak field branch (Morin et al. 2011). Stars on the strong (weak) field branch will have fields similar to stars in region 3 (1). V2247 Oph lies in this region and on the weak field dynamo branch.

The general magnetic topology characteristics of a given T Tauri star will change with age as the star evolves down its mass track toward the MS. In the high- and intermediate-mass regimes, stars with mass $\gtrsim 0.5 M_{\odot}$, T Tauri stars initially host magnetic fields that are axisymmetric with a strong dipole component. As the fully convective phase of evolution ends and a small radiative core develops the field remains largely axisymmetric but the dipole component decays away, leaving a field that is dominated by strong high-order field components (those with $\ell > 1$). By the time that the core mass exceeds $M_{\text{core}}/M_* \approx 0.4$ the dipole component is weak, and the field is complex having lost its earlier axisymmetry. This core mass boundary is empirical, based on the limited sample of stars where magnetic maps have been published to date, and is therefore somewhat speculative at this stage. Clearly more data are required to confirm the exact value, but we note that currently unpublished data are consistent with these trends. The boundary may be more fluid and itself dependent on stellar mass given that for higher mass stars the growth rate of the radiative core is more rapid than for lower mass stars (see Appendix B). Furthermore, if the boundary between fully convective stars with simple fields and those in the bistable regime is as extreme as masses below 60% of the fully convective limit (see the discussion in Section 3.3 and the left-hand blue dashed line in Figure 4) then this picture would have to be modified, as some stars would be born within the bistable regime and host fields with weak dipole components which would then strengthen as the stars approach the fully convective limit. It is not clear what interplay between the stellar contraction, rotation period, and mass could influence the dynamo process in this way.

The general T Tauri magnetic topology trends are currently empirical and are based on knowledge garnered from observationally derived magnetic maps. However, a magnetic topology change due to the transition from a fully to a partially convective stellar interior is further supported by the observed changes in periodic variability and X-ray luminosities (Rebull et al. 2006; Saunders et al. 2009; Mayne 2010). If ZDI data acquired in future continue to follow the empirical trends, then in principle it is possible to infer the general properties of a T Tauri star's large-scale magnetic field solely from its position in the H-R diagram.

We do not claim that it is possible to know the exact properties of a star's magnetic field based solely on its effective temperature and luminosity. Indeed we expect that the large-scale field topology, and the strength of the various magnetic field components, will evolve in time due to magnetic cycles (see Donati et al. 2011a, 2011b, 2012 for discussion about the changes in the fields on V2129 Oph, TW Hya, and GQ

Lup, although longer timescale observing programs potentially spanning several years are required to search for and confirm the existence of magnetic cycles on T Tauri stars). Nonetheless, it appears as though it is possible to estimate the general properties of the stellar magnetosphere, for example, whether or not the field will be dominantly axisymmetric with a weak dipole component, or axisymmetric with strong higher order components, or if the field will be highly complex with many multipolar components and non-axisymmetric. Our ability to do so, however, depends on both the accuracy with which the star has been positioned in the H-R diagram and on the veracity of the PMS stellar evolution models.

4.2. Limitations: Observational and Theoretical

Our ability to ascertain the magnetic topology of a given star from the H-R diagram would be limited by how well we can position the star in the H-R diagram and on the dependability of the PMS evolution models (see Hillenbrand et al. 2008 for a detailed review). Observationally the challenges lie in the assignment of a stellar spectral type, and the subsequent conversion to effective temperature with the assumption of some metallicity and surface gravity dependent scale. Likewise to discern the stellar luminosity we must carefully account for extinction, the presence of large surface cool spots and the related photometric variability, for accreting PMS stars the additional luminosity from accretion, uncertainties in the distance estimate, and for some sources the existence of unresolved close companions (Hartmann 2001).

Theoretically, the errors that can arise from assumptions in the constituent input physics of the PMS evolution models have been succinctly summarized by Siess (2001), Palla (2001), and Tognelli et al. (2011), with the latter paper providing detailed comparison between different evolutionary models. Modeling the evolution of a forming star along its mass track and across the H-R diagram is a formidable task. Errors, as well as differences between the various available PMS evolution models, arise from differing assumptions about the equation of state; the adopted boundary conditions, for example, whether a gray or more realistic atmosphere model is employed; how convection is handled; the assumed metallicity; the effects of mass accretion and rotation; and the influence of different formation histories during the protostellar phase. Taking these effects into account, Siess (2001) estimates the errors in the mass tracks to be $\Delta T_{\text{eff}} \sim 100\text{--}200\text{ K}$ and $\Delta \log(L_*/L_{\odot}) \sim 0.1$. Additionally, if magnetic fields themselves are not accounted for in models of convection, a further source of error is introduced to the models (D'Antona et al. 2000). Finally, most models do not account for episodic accretion which may alter the stellar structure and the age at which stars of a given mass develop a radiative core (Baraffe & Chabrier 2010).

The uncertainty in the stellar evolution models themselves, and the observational difficulty in accurately assigning effective temperatures and luminosities, must be kept in mind when using Figure 4 to predict the general magnetic field properties of a particular T Tauri star. However, turning the problem around, rather than using the star's position in the H-R diagram to ascertain its magnetic topology, it may be possible to use the observationally derived magnetic topology to test the accuracy of certain aspects of the PMS evolution models themselves. Just as dynamical mass measurements for binary stars (Palla & Stahler 2001; Hillenbrand & White 2004) and for single stars with disks (Simon et al. 2000) can be used to constrain the accuracy of mass tracks, and the amount of lithium depletion

isochronal ages (e.g., Palla et al. 2005; Soderblom 2010), magnetic field topologies may be used to test stellar internal structure information. For example, in Section 4.1 we argued that the field topology of T Tauri stars varies from simple and axisymmetric with a strong dipole component to complex and highly non-axisymmetric with a weak dipole component with the growth of a radiative core. A difference in the external field topology is expected given the different dynamo process operating in fully convective stars compared to more evolved and/or more massive stars with outer convection zones, radiative cores, and stellar analogs of the solar tachocline. The right-hand solid blue line in Figure 3 denotes the fully convective limit. By carrying out ZDI studies for stars around this limit, stark variation in the field topology between various stars may be used as a probe to observationally constrain which regions of the H-R diagram are populated by fully convective stars, and which regions are populated by stars with radiative cores. In other words, by determining the regions of the H-R diagram where stars with simple and complex magnetic fields lie, we can determine whether or not the internal structure information derived from the PMS evolution models is accurate.

5. DISCUSSION

5.1. The Dipole Component of T Tauri Magnetospheres and the Star–Disk Interaction

For accreting T Tauri stars it is generally the strength of the dipole component that is the most significant in terms of controlling the disk truncation radius, even when the dipole component is weak compared to the higher order components (Adams & Gregory 2012). This can be seen by considering the field strength at the inner disk truncation radius. Let’s consider a simple example of a star with a dipole plus an octupole field component, as many accreting T Tauri stars host large-scale magnetic fields of this form (Gregory & Donati 2011). In the equatorial plane the contribution to the vertical component of \mathbf{B} threading the disk at a distance r from the stellar center from the dipole component of polar strength B_{dip} is $B_{\text{dip}}(R_*/r)^3/2$. For the octupole field component the equivalent expression is $3B_{\text{oct}}(R_*/r)^5/8$, where B_{oct} is the polar strength of the octupole (Gregory et al. 2010). Thus, assuming a typical disk truncation radius of $5 R_*$ (which is $\sim 70\%$ of the equatorial corotation radius for a $2 R_\odot$ solar mass star with a rotation period of 6 days), then the ratio of the strength of the octupole to the dipole component at the inner disk edge is $(3/100)(B_{\text{oct}}/B_{\text{dip}})$. Taking the ratio of the polar strength of the field components as $B_{\text{oct}}/B_{\text{dip}} = 10$, which is larger than thus far observed for any T Tauri star (which is $B_{\text{oct}}/B_{\text{dip}} \approx 6$ for TW Hya in 2008 March; Donati et al. 2011b) then the contribution to the field at the inner disk from the octupole component is only 30% that of the dipole component, and becomes less significant the weaker (stronger) the octupole (dipole) component and for larger disk truncation radii.¹¹ The dipole is, in the majority of cases, the most significant field component in controlling the disk truncation radius.

Figure 5 shows the variation in the polar strength of the dipole component for high- and intermediate-mass T Tauri stars listed in Table 2. It is clear that more massive and/or older T Tauri stars, those which have ended the fully convective phase of evolution, have weaker dipole components than younger and/or

lower mass stars. A possible exception is for some of the low-mass T Tauri stars which may show a variety of field topologies (see Section 3.3).

The observed rapid decay in the dipole component with the growth of a radiative core can influence the star–disk interaction only if the fully convective phase ends before the disk has dispersed. As demonstrated in Appendix B the age at which a radiative core develops is highly dependent on stellar mass, with high-mass T Tauri stars ($\gtrsim 1.0 M_\odot$) ending the fully convective phase in $\lesssim 2.6$ Myr based on the Siess et al. (2000) models, or $\lesssim 2.2$ Myr based on the Tognelli et al. (2011) models. This timescale drops to as little as 0.5 Myr in both models for stars of $2 M_\odot$. Therefore the drop in the dipole component, and the subsequent effect on the star–disk interaction, is more relevant for higher mass T Tauri stars than for lower mass stars as most of the latter will have lost their disks before the end of the fully convective phase. However, there is also observational evidence that the disk lifetime is mass dependent with high-mass stars losing their disks faster than stars in the intermediate- and low-mass ranges (Carpenter et al. 2006; Currie & Kenyon 2009; Williams & Cieza 2011).¹² Therefore, the effect of the evolution of the large-scale stellar magnetic field topology becomes a question of timescales. For a given star does the radiative core develop before it stops interacting with its circumstellar disk? There are a number of well-studied T Tauri stars in the high- and intermediate-mass ranges which have developed radiative cores and which show evidence for significant ongoing accretion and substantial disks, for example, the stars discussed in this paper as well as those studied by Calvet et al. (2004).

In principle, the rapid drop in the dipole component, and therefore the field strength at the inner disk, at the end of fully convective phase will allow the disk to push closer to the star. This would lead to a increased spin-up torque acting on the star due to the magnetic links with the disk interior to the equatorial corotation radius that are rotating faster than the star (in addition to the spin-up torques from accretion and the stellar contraction; Matt & Pudritz 2005) and consequently an increase in the stellar rotation rate. In contrast, fully convective stars (at least those that are not in the weak field bistable dynamo regime) with strong dipole components should be able to maintain their slow rotation by truncating their disks out to, and perhaps even beyond, the corotation radius (the propeller regime; Romanova et al. 2004b; Donati et al. 2010b).

There is tentative evidence for this rotational evolution scenario within the sample of stars considered in this paper. In Figure 3, the size of the symbols is proportional to the rotation period of the star (listed in Table 2). For intermediate- and high-mass T Tauri stars ($> 0.5 M_\odot$) the fully convective stars which have strong dipole components are more slowly rotating than those which have ended the fully convective phase. Additionally, stars which have spent longer with radiative cores (and therefore with weak dipole components) are, on average, rotating faster than the fully convective stars. This strongly hints that the effect of the change in the magnetic topology with the development of a radiative core is that a PMS star enters a spin-up phase, if they are still interacting with their disks when this transition occurs. However, this picture may be too simplistic, as the disk truncation radius is sensitive to parameters other than the

¹¹ This simple illustrative example ignores the tilt of the multipole components which should be accounted for when calculating the field strength at the inner disk, and consequently the disk truncation radius (Gregory et al. 2008).

¹² Recent theoretical models suggest only a weak stellar mass dependence on disk lifetimes (Gorti et al. 2009; Ercolano et al. 2011). Furthermore, disk lifetimes may be influenced by the star-forming environment (Luhman et al. 2008).

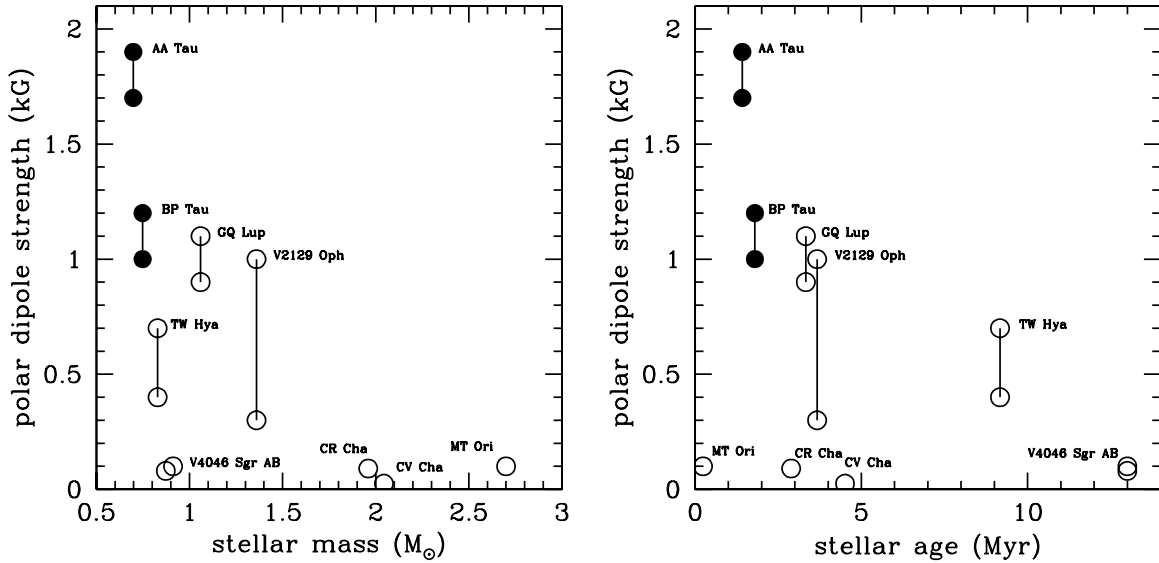


Figure 5. Polar strength of the dipole component of the magnetic fields of various accreting T Tauri stars as a function of stellar mass (left) and age (right) in the intermediate- and high-mass ranges ($\gtrsim 0.5 M_{\odot}$) listed in Table 2. Filled circles denote fully convective stars, and open circles stars with radiative cores, as determined from the PMS evolution models of Siess et al. (2000). The solid vertical lines join the same star observed at two different epochs. It is clear that higher mass and/or older stars have weaker dipole components than lower mass and/or younger stars.

magnetic field strength which will vary with time, and disk lifetimes are likely also a function of many parameters.

The disk truncation radius depends on the stellar radius, the mass accretion rate, and the polar strength of the stellar dipole component $R_t \propto B_{\text{dip}}^{4/7} R_*^{12/7} \dot{M}^{-2/7}$ (e.g., König 1991).¹³ Although a drop in the dipole component will allow the disk to push closer to the star (as will the reduction in the stellar radius, since PMS stars are contracting), the observed drop in mass accretion rate with increasing stellar age (e.g., Hartmann et al. 1998; Sicilia-Aguilar et al. 2004) has the opposite effect and allows the stellar magnetosphere to keep the disk at bay at a larger radius. Thus, the disk truncation radius, and consequently the balance of torques in the star–disk system, will depend on the interplay between the rate of decay of the dipole component and the drop in the mass accretion rate with time. Additionally, magnetic cycles (the beginnings of which may have already been observed in V2129 Oph and GQ Lup, see Appendix A) will cause variations in the large-scale field topology, and therefore the disk truncation radius, over time. Thus, a new generation of magnetospheric accretion models that track the rotational evolution of the star incorporating the time evolution of the mass accretion rate, the stellar contraction (similar to those of Matt et al. 2010, 2012) and for the first time the time evolution of magnetic fields following the observational correlations and magnetic cycles are now warranted.

5.2. Magnetic Field Topology, Rotation Rate, and Rossby Number

Throughout this paper we have concentrated on the links between the stellar mass and age, which considered in tandem reveal the stellar internal structure and the large-scale magnetic

field topology. However, the stellar rotation rate and the Rossby number, the ratio of the rotation period to the local convective turnover time in the stellar interior ($\text{Ro} = P_{\text{rot}}/\tau_c$), may also influence the magnetic topology. In order to search for such trends we require estimates of the convective turnover time τ_c . As PMS stars are contracting, and especially once a radiative core begins to grow at the expense of the convective zone depth, τ_c values are highly sensitive to the stellar mass and age. Unfortunately, most published τ_c estimates come from models that track the stellar evolution over timescales of order Gyr and across a limited range of stellar mass (Gilliland 1986; Kim & Demarque 1996; Landin et al. 2010), and lack the time and mass resolution required for our purposes. An exception is the model of Jung & Kim (2007). Y.-C. Kim has kindly supplied us with finer resolution grids than published. Our rough convective turnover time estimates are listed in Table 1. The τ_c values are calculated at a distance of half of the mixing length above the base of the convective zone. Although it is only an assumption that this is the depth where the dynamo operates, the same assumption is made in the cited models and is fully consistent with the work of others (e.g., Johns-Krull et al. 2000; Preibisch et al. 2005; Alexander & Preibisch 2012).

Zeeman broadening studies (e.g., Johns-Krull 2007) have found no links between the mean surface magnetic field strengths of PMS stars and rotation parameters. This is perhaps not surprising given that all T Tauri stars lie in the saturated regime (with some into the supersaturated regime) of the well-defined MS rotation–activity relation: plots of the ratio of X-ray to bolometric luminosity versus Rossby number (Preibisch et al. 2005). Zeeman broadening, which probes all of the small-scale magnetic field regions close to the star (the tangling and reconnection of which gives rise to the X-ray emission), does not give access to information about the large-scale field topology. In this work, we are particularly interested in links between the rotation parameters and the polar strength of the dipole component, given its importance to the star–disk interaction (see Section 5.1).

In Figure 6, we present plots of B_{dip} versus the rotation parameters (P_{rot} and Ro ; plots with $v_* \sin i$ as the abscissa,

¹³ There is a difference in R_t for multipolar compared to dipolar magnetospheres, although in most cases this difference is small (see Section 6 of Adams & Gregory 2012). Provided that the dipole component is not significantly tilted with respect to the stellar rotation axis, R_t values can be estimated using the strength of the dipole component at the stellar rotation pole. The higher order field components, however, must be accounted for in models of accretion flow onto the star (Gregory & Donati 2011; Adams & Gregory 2012).

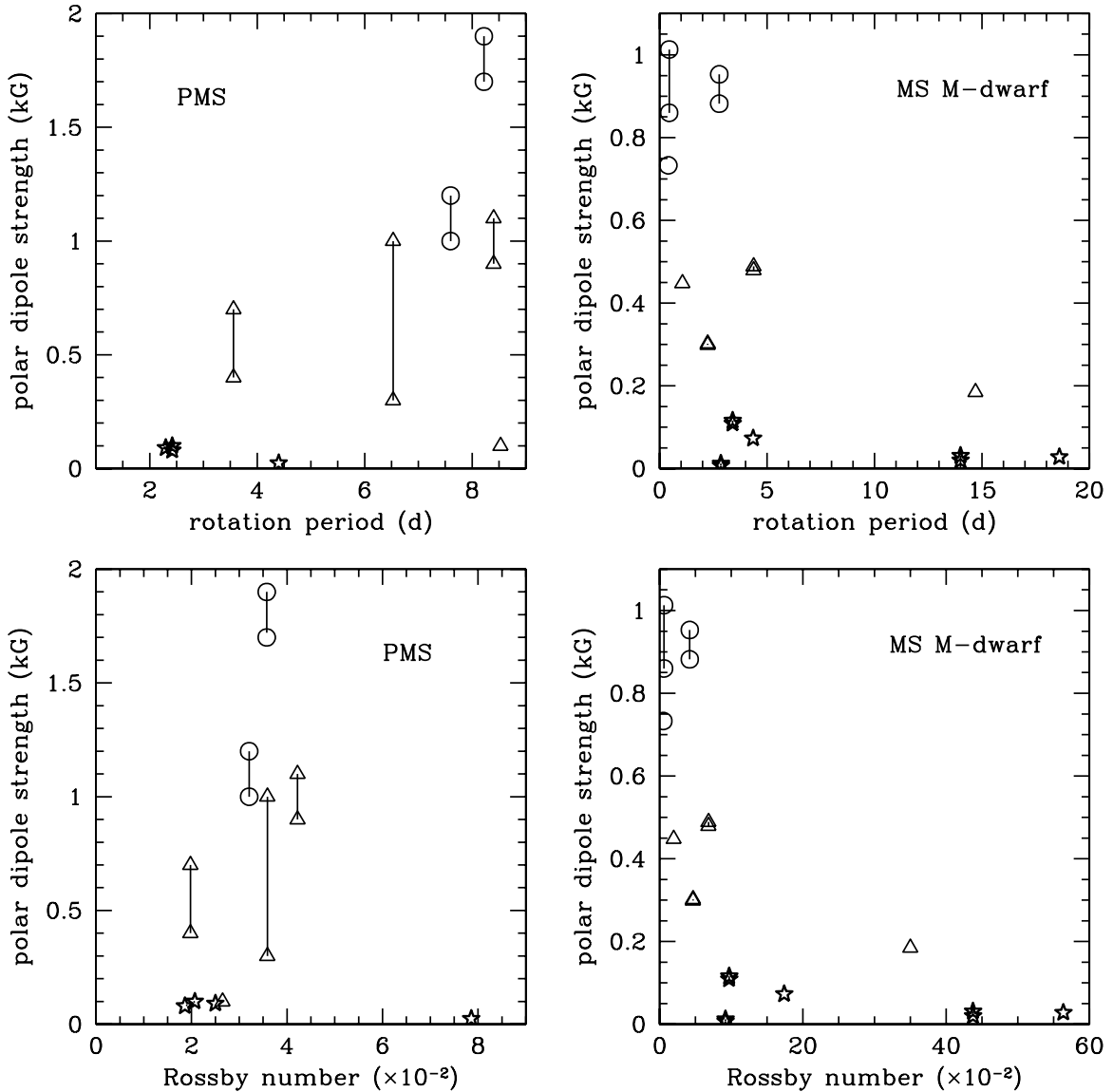


Figure 6. Polar strength of the dipole component of the multipolar magnetic fields of the intermediate/high-mass PMS stars (left) and MS M-dwarfs (right; early/mid-M spectral types from Donati et al. 2008b and Morin et al. 2008) vs. rotation period (upper) and Rossby number (lower). Points connected by vertical lines are stars observed at two epochs. Circles are fully convective stars, triangles (asterisks) stars with small (large) radiative cores.

which are not shown, are similar to the P_{rot} plots) for both intermediate/high-mass PMS stars and the early/mid-spectral-type MS M-dwarfs from Morin et al. (2008) and Donati et al. (2008b). The M-dwarf sample spans the unsaturated and saturated regimes of the rotation–activity relation (Donati et al. 2008b). The saturated regime occurs at rotation periods of $P_{\text{rot}} \lesssim 4$ days for M-dwarfs of mass $\sim 0.5 M_{\odot}$, or at $\text{Ro} \lesssim 0.1$ (Pizzolato et al. 2003). M-dwarfs which lie in the saturated regime (like all PMS stars) show little relation between P_{rot} and B_{dip} with a range of polar dipole strengths, being strongest for the fully convective stars (lowest mass; circles in Figure 6, upper right panel), weakest for the stars with small outer convective zones (highest mass; asterisks), and of intermediate strength for stars slightly more massive than the MS fully convective limit (triangles), as already discussed—see Figure 2.¹⁴ There do appear to be correlations between B_{dip}

and P_{rot} , and B_{dip} and Ro , for MS M-dwarfs if the sample is considered as a whole. The latter trend is driven by the factor of ~ 10 range of P_{rot} values across the sample rather than the range of τ_c values, which vary by a factor of ~ 2 (as listed in Donati et al. 2008b and Morin et al. 2008), with the overall correlations arising as all the observed fully convective stars (circles in Figure 6 right panel) and almost all stars which are mostly convective (triangles) are faster rotators, while substantially radiative stars (asterisks) span a range of rotation rates.

There is a clearer link between B_{dip} and P_{rot} for the PMS sample with the stars with the strongest dipole components (fully convective stars) spinning more slowly than stars with weaker dipole components (stars with radiative cores)—see Figure 6. This is likely being driven by the star–disk interaction with stars with stronger dipole components able to truncate their

¹⁴ Morin et al. (2011), their Figure 2, and Donati (2011), his Figure 1, provide more complete overviews of the links between mass, rotation period, field topology, and Rossby number for MS stars. Such plots of the $M_* - P_{\text{rot}}$ plane with contours of constant Ro are not meaningful for our small sample of PMS

stars, which span a range of stellar ages, as the Ro contours are highly sensitive to age due to the variation of τ_c values with the stellar contraction and radiative core growth.

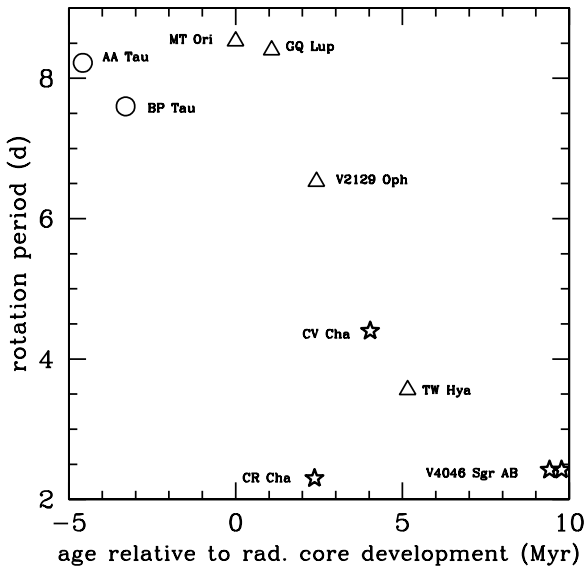


Figure 7. Stellar rotation periods for the intermediate/high-mass accreting PMS stars as a function of time since (positive abscissa values) or time until (negative abscissa values) the development of a radiative core. The symbols are as in Figure 6. Stars which have spent longer with radiative cores (and therefore with weaker dipole components; see Figure 5) are faster rotators.

disks out to corotation, see Section 5.1, and those with weaker dipole components having smaller disk truncation radii and therefore being spun-up. GQ Lup and MT Ori (the rightmost three triangles in Figure 6) are not exceptions to this trend, as these stars have only recently ended the fully convective phase and presumably have not had enough time to spin up. This argument is supported by the strong correlation in Figure 7 where we have estimated the time relative to the end of the fully convective phase (that is the age of a star minus the age at which a star of its mass is expected to develop a radiative core as calculated from Equation (B1)). It is clear that the longer a star has spent with a radiative core, the faster its rotation rate.¹⁵

We suggest that the relation between the stellar rotation rate and the strength of the dipole component for PMS stars is driven by the star–disk interaction rather than the dynamo magnetic field generation process itself. This is further supported by the lack of any clear relation between B_{dip} and Rossby number, see Figure 6 (lower left panel). Although τ_c values drop from a couple of hundred days to a few tens of days with the development of a large radiative core (e.g., Jung & Kim 2007), P_{rot} values are also smaller for stars with large cores (see the asterisks in Figure 6, upper left panel). Thus, there is little variation in Ro across our PMS sample, all of which lie in the saturated regime of the rotation–activity relation. Likewise, there is little variation in Ro values for MS M-dwarfs that lie in the saturated regime ($Ro \leq 0.1$).

5.3. Non-accreting Pre-main-sequence Stars

Given the importance of magnetic fields in controlling the star–disk interaction, and in turn the stellar rotational evolution, we have thus far focused our discussion on accreting T Tauri stars. Magnetic maps have also been published for one non-accreting weak-line T Tauri star, V410 Tau (Skelly et al. 2010),

¹⁵ The trend in Figure 7 is unlikely to be caused (at least entirely) by the stellar contraction, that is by the spin-up of stars as they contract with age in order to conserve angular momentum—there is no clear trend between P_{rot} and R_* across our sample. Furthermore, stars in Figure 7 on either side of the fully convective divide span a range of ages.

and a handful of post T Tauri stars that have long since lost their disks and have spun-up, HD 155555 (a close binary system; Dunstone et al. 2008a), HD 141943 (Marsden et al. 2011), and HD 106506 (Waite et al. 2011). With the exception of V410 Tau all of the non-accreting stars have substantial radiative cores ($M_{\text{core}}/M_* \approx 0.93$ and ≈ 0.84 for the primary and secondary stars of HD 155555) or have entirely radiative interiors (HD 106506 and HD 141943) as inferred from the models of Siess et al. (2000). The non-accreting T Tauri stars are typically faster rotators than the accreting stars considered in Section 2 with $P_{\text{rot}} \leq 2.2$ days, as is commonly found (e.g., Bouvier et al. 1993). The post T Tauri stars have small, or no, outer convective zones and are found to host highly complex magnetic fields with many high-order field components. This is consistent with the magnetic evolutionary scenario discussed above for accreting T Tauri stars.

V410 Tau is the only non-accreting star with a small radiative core for which magnetic maps have been obtained (Skelly et al. 2010). It is a young (~ 1.7 Myr) and higher mass star ($M_* \approx 1.4 M_\odot$). Widely varying estimates of its effective temperature have been reported in the literature, and its luminosity is highly uncertain given the large spot coverage (see the discussion in Skelly et al. 2010). Thus, the position of V410 Tau in the H-R diagram is poorly constrained. According to the models of Siess et al. (2000) this star has already ended the fully convective phase of evolution and has a small radiative core ($M_{\text{core}}/M_* \approx 0.07$), although given the uncertainty in its H-R diagram position it may have an internal structure that ranges from fully convective to having a moderately sized core ($M_{\text{core}}/M_* \approx 0.3$; Skelly et al. 2010). Its complex magnetic field topology has more in common with the accreting T Tauri stars with large radiative cores, suggesting that it has indeed ended the fully convective phase. However, with only one genuine weak-line T Tauri star studied thus far it is not clear if the magnetic fields of these stars will follow similar trends as found for accreting classical T Tauri stars; but given that accreting stars (of age a few Myr) follow a similar magnetic topology trend with internal structure as found for MS M-dwarfs (of age a few Gyr), it is reasonable to assume that the magnetic topologies of more evolved PMS stars will follow suit. If they do not, it may indicate that accretion is modifying the stellar magnetic field generation process. Furthermore, if our conclusion that it is the star–disk interaction that is driving the relation between P_{rot} and B_{dip} (see Section 5.2 and Figure 6, upper left panel) is correct then we do not necessarily expect to find the same behavior for systems where the disk has dispersed. With the influence of the disk removed, underlying relationships between the stellar magnetic field topology and the dynamo properties may be revealed. Non-accreting T Tauri stars will be the target of future spectropolarimetric observing campaigns to specifically address such issues.

6. CONCLUSIONS

Spectropolarimetric observations carried out over at least a full stellar rotation, and ideally several rotation periods, combined with tomographic imaging techniques have allowed maps of the magnetic fields of a small sample of accreting T Tauri stars to be derived (Donati et al. 2007, 2008a, 2010a, 2010b, 2011a, 2011b, 2011c, 2012; Hussain et al. 2009; Skelly et al. 2012). T Tauri magnetic field topologies are found to vary with the stellar parameters. We find that the large-scale topology appears to be directly linked to the internal structure of the star,

and in particular to the size of the radiative core that develops at the end of the fully convective phase of evolution.

We define four regions across the H-R diagram, see Section 4.1 and Figure 4, delineating stars with different magnetic topology characteristics. Stars with substantial radiative cores, $M_{\text{core}}/M_* \gtrsim 0.4$, have complex fields that are highly non-axisymmetric with weak dipole components, only a few tenths of a kG at most (this defines region 1 of the H-R diagram as discussed in Section 4.1 and colored blue in Figure 4). V4046 Sgr AB, CR Cha, and CV Cha have this type of field topology. Stars which have small radiative cores, $0 < M_{\text{core}}/M_* \lesssim 0.4$, have largely axisymmetric large-scale magnetic field topologies but field modes of higher order than the dipole component dominate. Their dipole components are generally weaker than those found for fully convective stars and appear to range from less than 0.1 kG to around 1 kG. MT Ori, TW Hya, V2129 Oph, and GQ Lup possess magnetic fields like this. Intriguingly, stars that fall in this region of the H-R diagram (region 2 discussed in Section 4.1 and colored green in Figure 4) for which magnetic maps have been published all have strong octupole components to their magnetic fields, and this is the dominant field mode in TW Hya, V2129 Oph, and GQ Lup. There are currently no theoretical models to explain this trend.

We emphasize that the limit of $M_{\text{core}}/M_* \approx 0.4$ between the regions 1 and 2 is empirical and more observations are required to properly determine the exact boundary. The boundary may also be a function of stellar mass itself, but we note that for MS M-dwarfs (whose topology trends with stellar internal structure mirror the behavior of PMS stars) the transition from dominantly axisymmetric to dominantly non-axisymmetric fields occurs at $M_* \sim 0.5 M_{\odot}$ (see Figure 1) which (roughly) corresponds to $M_{\text{core}}/M_* \approx 0.4$.

Fully convective stars of mass $\gtrsim 0.5 M_{\odot}$ host simple fields that are dominantly axisymmetric with strong dipole components of order one to a few kG (region 3 of the H-R diagram as discussed in Section 4.1 and colored yellow in Figure 4). AA Tau and BP Tau fall into this category. Such stars will develop radiative cores before they arrive on the MS, at which point it seems likely that the dipole component of their magnetic fields will decay, but initially the axisymmetric nature of their fields will be maintained. Further core growth will eventually destroy the axisymmetry of their magnetic fields leaving the stars with complex fields with weak dipole components. It appears as though this drop in the dipole component, which will reduce the disk truncation radius and increase the spin-up torque on the star, influences the stellar rotation rate with stars which have spent longer with radiative cores being faster rotators.

Although the magnetic topology trends that we have observed across the PMS of the H-R diagram (see Figures 3 and 4) are thus far based on a limited sample of stars, it is the overall excellent agreement between the large-scale field topologies of PMS stars and those of MS M-dwarfs with comparable internal structures (i.e., similar ratios of core mass to stellar mass M_{core}/M_*) that gives us confidence to define distinct magnetic topology regimes. Further spectropolarimetric studies of PMS stars across the H-R diagram are now required to test our conclusions. By far the clearest trends, observed for both the MS and PMS sample, is the rapid increase in field complexity, and the rapid decrease in the dipole component, when moving from objects close to the fully convective divide to those with substantial radiative cores.

The lowest mass M-dwarfs (below $\sim 0.2 M_{\odot}$, or later than spectral type $\sim M5$) are found to host a variety of field topologies

which may be due to a bistable dynamo process (Morin et al. 2010, 2011). The similarity between the field topologies of MS M-dwarfs and PMS stars allows us to predict that bistable dynamo behavior, and therefore stars with a variety of large-scale field topologies, will be found for the lowest mass PMS stars. We have thus defined a fourth region of the H-R diagram where such stars will be found. The exact boundary between this region 4 and region 3 is poorly constrained and more ZDI studies are required for stars in this low-mass regime. The only star studied in this region thus far is V2247 Oph, a fully convective star with a complex field that likely resides on the weak field bistable dynamo branch (stars on the strong field branch would host simple fields).

Although the magnetic topology trends with stellar internal structure are empirical and currently lack theoretical grounding, there is additional evidence for a field topology change as stars transition from fully to partially convective. With the growth of a radiative core large-scale magnetic fields become more and more complex. Saunders et al. (2009) argued that such a change could explain their observed reduction in the number of periodically variable PMS stars, with fully convective stars hosting simple fields with large cool spots and partially convective stars more complex fields with more numerous and distributed smaller spots (which causes less photometric rotational variability). This is fully consistent with the Doppler maps of fully convective T Tauri stars which often show large (usually slightly offset from the rotation pole) high-latitude spots (e.g., Donati et al. 2010b). Likewise Rebull et al. (2006) and Mayne (2010) find a systematic reduction in the ratio of X-ray to bolometric luminosity, which is driven by the strength of the convective dynamo, for stars with radiative cores. Furthermore, Alexander & Preibisch (2012) argue that the change from fully to partially convective stellar interiors can explain their observation that the scatter in X-ray luminosities in rotation–activity plots reduces with increasing PMS cluster age. While these observations lack the clarity or precision of our own, they do add significant support to the change in magnetic field topology that we observe.

We conclude that it is possible to predict the general characteristics of the magnetic field of a PMS star based purely on its position in the H-R diagram. For example, whether the field will be axisymmetric with a strong dipole component, or axisymmetric with a field component of higher order than the dipole dominant, or complex and non-axisymmetric with a weak dipole component. Large-scale magnetic field topologies are likely variable over time too, as has been observed for V2129 Oph, TW Hya (tentatively), and GQ Lup (Donati et al. 2011a, 2011b, 2012). However, although the polar strength of the various field components was observed to vary for all of these stars, the general characteristics of their large-scale fields remained the same at both epochs—dominantly octupolar and well described by a tilted dipole plus a tilted octupole component (Gregory & Donati 2011). Likewise the general properties of the magnetic fields of AA Tau and BP Tau remained the same as derived from data sets taken in different observing seasons.

We do caution, however, that our ability to predict the general large-scale magnetic topology characteristics of a given PMS star is reliant on the veracity of the PMS evolution models themselves and on our ability to accurately position the star in the H-R diagram in the first place. An alternative point of view, however, is that we can use ZDI studies and the derived magnetic topologies of T Tauri stars as a direct test of the internal structure information derived from the PMS evolutionary models themselves, just as dynamical mass

measurements can constrain the mass tracks (Hillenbrand & White 2004) and lithium depletion the isochrones (Palla et al. 2005). For example, if a star is found to host a largely axisymmetric field, but with dominant high-order components, it is likely that this star has already ended the fully convective phase of evolution and has developed a small radiative core. If the star falls in a region of the H-R diagram where fully convective stars lie, it could then be argued that either the models are inadequate in this region, and/or a better assignment of the stellar effective temperature and luminosity needs to be made.

In principle, ZDI studies can be used to provide strong observational constraints on the divide between the fully and partially convective regions of the PMS in the H-R diagram; a divide that is exquisitely model dependent. Pinpointing this divide observationally should allow the detailed testing of evolutionary models of stellar internal structure. Observationally constraining the fully convective divide as a function of mass and age does not only have important implications for periodic variability and X-ray emission, as discussed above. Additionally, the development of a radiative core likely leads to a dramatic redistribution of angular momentum as the convective envelope and core decouple (Endal & Sofia 1981), which, if further studied, should yield insights into such phenomena as rotationally induced mixing (e.g., Pinsonneault 1997). Furthermore, as the interaction with a circumstellar disk is (in most, but crucially not all, cases) dominated by the large-scale dipole component of the magnetic field (Gregory et al. 2008; Adams & Gregory 2012), studying stars with disks across the fully convective/radiative core divide will enable us to probe the dynamics and physics of magnetospheric accretion as a function of magnetic field topology in an extremely targeted fashion.

Data from the MaPP program will continue to be obtained until at least the end of 2012. This continued stream of T Tauri magnetic maps, coupled with those for stars already observed as part of MaPP but not yet published, will allow the H-R diagram to be more fully populated. This will allow the boundaries separating the different topology regions within the H-R diagram to be better constrained observationally. Furthermore, by repeatedly observing the same stars over timescales of several years we will gain insight into the long-term variability of the large-scale magnetospheres of T Tauri stars, and possibly the existence of magnetic cycles. MaPP will thus further advance our understanding of the magnetism of forming low-mass, including solar-like, stars. From a theoretical perspective models of the magnetospheric accretion process that incorporate magnetic fields with an observed degree of complexity have been developed (Gregory et al. 2005, 2006, 2008, 2010; Long et al. 2008, 2011, 2012; Mohanty & Shu 2008; Romanova et al. 2011; Gregory & Donati 2011; Adams & Gregory 2012). However, the observed variations in the magnetic field topology with the development of a radiative core, and the possible bistable dynamo process that appears to operate among the lowest mass T Tauri stars, highlight the need for new models, similar to those of Matt et al. (2010, 2012), but which take proper account of both the magnetic field complexity and the field variation with changes in the stellar internal structure.

The authors thank L. Siess, N. Baliber, and F. C. Adams for insightful discussions, E. Tognelli and P. G. Prada Moroni for sending stellar internal structure information from their PMS evolution models, Y.-C. Kim for sending convective turnover time estimates, and the referee for useful comments. S.G.G.

is supported by NASA grant HST-GO-11616.07-A. J.M. is supported by a postdoctoral fellowship of the Alexander von Humboldt foundation. The “Magnetic Protostars and Planets” (MaPP) project is supported by the funding agencies of CFHT and TBL (through the allocation of telescope time) and by CNRS/INSU in particular, as well as by the French “Agence Nationale pour la Recherche” (ANR).

APPENDIX A

ACCRETING T TAURI STARS WITH MAGNETIC MAPS DERIVED FROM ZDI

A.1. Stars with Strong Dipole Components and Axisymmetric Large-scale Magnetic Fields

A.1.1. AA Tau

AA Tau is one of the best-studied accreting stars and hosts the simplest large-scale magnetic field yet discovered on any T Tauri star. Its large-scale field is dominantly dipolar, with weak high-order field components (Donati et al. 2010b). The dipole component is strong with a polar field strength of ~ 2 kG (perhaps as large as 3 kG, see the discussion in Donati et al. 2010b) and is tilted by $\sim 10^\circ$ – 20° with respect to the stellar rotation axis, see Table 2. The star was observed at two different epochs separated by a year. The large-scale field topology showed no significant evolution, which may be linked to the moderate phase coverage obtained at both epochs, but repeat observations are required to confirm this. Given the weak mass accretion rate onto AA Tau during the ESPaDOnS observations (an average of $\log \dot{M} = -9.2 M_\odot \text{ yr}^{-1}$; Donati et al. 2010b) coupled with the strength of the dipole component the disk may be truncated close to the equatorial corotation radius, or even beyond at some epochs. The mass accretion rate, however, was observed to vary by an order of magnitude from $\log \dot{M} = -9.6$ to $-8.5 M_\odot \text{ yr}^{-1}$. AA Tau has a completely convective interior according to both the Siess et al. (2000) and the Tognelli et al. (2011) PMS stellar evolution models.

A.1.2. BP Tau

BP Tau has long been known to possess a strong stellar-disk-averaged magnetic field from Zeeman broadening measurements (Johns-Krull et al. 1999b), with strong circular polarization measured in the accretion-related He I 5876 Å emission line (Johns-Krull et al. 1999a; Symington et al. 2005; Chuntunov et al. 2007). Like AA Tau, ZDI has revealed that BP Tau has a strong dipole component to its magnetic field (Donati et al. 2008a). However, it also possesses a strong octupole field component (of polar field strength of 1.6–1.8 kG compared to the dipole component of polar field strength 1–1.2 kG; see footnote “c” of Table 2). Both the dipole and octupole moments are tilted relative to the stellar rotation axis, but by different amounts and toward different rotation phases. Magnetic maps have been derived at two different epochs, separated by around 10 months (Donati et al. 2008a). The large-scale field topology showed little change over this time, apart from an apparent rotation of the entire surface field by 0.25 in phase. This was most likely caused by a small error in the assumed rotation period (7.6 ± 0.1 days) building up over the ~ 39 rotations between the observing epochs. Variations in the large-scale field topology cannot, however, be ruled out on longer timescales. We further note that the magnetic maps for BP Tau were published prior to the MaPP project, using an experimental version of the magnetic imaging code (Donati et al. 2008a). This code considered

polarization signals in the photospheric absorption lines and the accretion-related emission lines separately, whereas the more mature version of the code constructs the maps by considering both signals simultaneously (Donati et al. 2010b). The archival spectropolarimetric observations of BP Tau will be re-analyzed in a forthcoming paper and will be presented alongside new recently obtained data. From its position in the H-R diagram BP Tau is a fully convective star.

A.2. Stars with Dominant High-order Magnetic Field Components and Axisymmetric Large-scale Fields

A.2.1. V2129 Oph

V2129 Oph was the first accreting T Tauri star for which magnetic maps were published (Donati et al. 2007; see also Donati et al. 2011a for a re-analysis of the original data set using the latest version of the magnetic imaging code). It has been observed at two different epochs, 2005 June and 2009 July (Donati et al. 2007, 2011a). At both epochs V2129 Oph was found to host a dominantly octupolar magnetic field. The dipole component of its multipolar magnetic field was found to vary by a factor of about three, from ~ 0.3 kG to ~ 1.0 kG, in the four years between the observing runs (Donati et al. 2011a). The clear detection of secular evolution of the large-scale magnetic field demonstrates that it is dynamo generated and not of fossil origin. At both epochs the dipole and octupole field components were found to be slightly tilted with respect to the stellar rotation axis and tilted toward different rotation phases. V2129 Oph has a binary companion (Ghez et al. 1993) although this is about 50 times fainter in the *V* band than V2129 Oph itself (Donati et al. 2007). The projected separation of $0''.65$, as measured by (Cieza et al. 2010), translates to 78 AU assuming a distance of 120 pc to the ρ Oph star-forming region (Loinard et al. 2008). V2129 Oph is no longer fully convective and has developed a small radiative core, $M_{\text{core}}/M_* \approx 0.2$ (Siess et al. 2000).

A.2.2. GQ Lup

GQ Lup was found to host a dominantly octupolar magnetic field when observed in both 2009 July and 2011 June (Donati et al. 2012). However, its large-scale field weakened considerably between the two observing epochs indicating a non-stationary dynamo process. The polar strength of the octupole component dropped from 2.4 kG to 1.6 kG and that of the dipole from 1.1 kG to 0.9 kG between 2009 and 2011. At both epochs the octupole was roughly aligned with the stellar rotation axis but the dipole component was tilted by $\sim 30^\circ$ (Donati et al. 2012). Of the stars for which magnetic maps have been derived to date, GQ Lup displays the strongest large-scale fields yet discovered, with the longitudinal field component measured in accretion-related emission lines (i.e., those which probe the field where accretion columns impact the star) reaching 6 kG. GQ Lup has a known substellar companion in its outer accretion disk, orbiting at ~ 100 AU (Neuhäuser et al. 2005), that is most likely a brown dwarf (Lavigne et al. 2009). GQ Lup has developed a small radiative core, $M_{\text{core}}/M_* \approx 0.13$ (Siess et al. 2000).

A.2.3. TW Hya

As with V2129 Oph and GQ Lup, TW Hya was found to host a dominantly octupolar magnetic field at the two epochs it was observed (Donati et al. 2011b). At both epochs the dipole component was found to be weak relative to the octupole component, with the ratio of their polar strengths varying from

$B_{\text{oct}}/B_{\text{dip}} \approx 6$ in 2008 March to $B_{\text{oct}}/B_{\text{dip}} \approx 4$ in 2010 March. At the first epoch the positive pole of the dipole component was found to be tilted by about 45° relative to the main negative pole of the octupole component. At the second epoch the dipole and octupole moments were roughly anti-parallel, with the main negative pole of the octupole coincident with the visible rotation pole of the star. The change in the tilt of the dipole component is tentative, however, given the relative weakness of the dipole component and the limited phase coverage obtained during the first observing run (Donati et al. 2011b). It may be indicative of a magnetic cycle, but clearly repeated observations, potentially over many years and with improved phase coverage, are required to confirm this. TW Hya is a somewhat atypical T Tauri star given its low inclination ($\approx 7^\circ$; Qi et al. 2004) and since it still has a significant mass accretion rate (averaging $\log \dot{M} = -8.9 M_\odot \text{ yr}^{-1}$ at both observing epochs; Donati et al. 2011b) despite being of an age (~ 9 Myr) where the disks of most T Tauri stars have dispersed and accretion has ceased (e.g., Fedele et al. 2010). TW Hya has an interior structure that consists of a radiative core surrounded by an outer convective envelope, with a core mass of $M_{\text{core}}/M_* \approx 0.2$ (Siess et al. 2000).

A.2.4. MT Ori

MT Ori hosts a complex magnetic field with the surface of the star covered in many regions of opposite polarity, although its large-scale field is dominantly axisymmetric (i.e., the $m = 0$ field modes dominate; Skelly et al. 2012). The large-scale dipole component was found to be weak < 100 G with the field dominated by the octupole ($\ell = 3$), the dotriacontapole ($\ell = 5$), and the $\ell = 7$ field modes. The total contribution from the $3 \leq \ell \leq 7$ field components was 13 times stronger than the dipole ($\ell = 1$) component with the octupole 4 times stronger than the dipole (Skelly et al. 2012). At $\sim 2.7 M_\odot$ according to the models of Siess et al. (2000), or $\sim 2 M_\odot$ using the models of Tognelli et al. (2011), and ~ 0.25 Myr this is the highest mass and youngest star in the MaPP sample. Despite its young age, MT Ori is massive enough to have already developed a small radiative core, at least in the models of Siess et al. (2000). The Tognelli et al. (2011) models suggest that MT Ori is still fully convective. Given the similarity of its magnetic field to that of TW Hya, V2129 Oph, and GQ Lup, stars which have small radiative cores in both PMS evolution models, and the dissimilarity between its field and the simple fields of the fully convective stars AA Tau and BP Tau, we suggest that MT Ori does indeed have a small radiative core. Given the large uncertainty in its effective temperature and luminosity (see Skelly et al. 2012) the core mass lies somewhere in the range $0.01 \leq M_{\text{core}}/M_* \leq 0.36$ according to the Siess et al. (2000) models.

A.3. Stars with Complex Non-axisymmetric Large-scale Magnetic Fields with Weak Dipole Components

A.3.1. V4046 Sgr AB

Both stars of the close binary system V4046 Sgr host complex magnetic fields with many high-order field components (Donati et al. 2011c). The large-scale magnetospheres of each star, their dipole components, are weak and highly tilted with respect to their rotation axes (of polar strength ~ 100 kG and ~ 80 kG and tilted by 60° and 90° on the primary and secondary, respectively). The planes of the tilts of the dipole moments are also offset by roughly 0.7 in rotation phase, further

Table 1
Fundamental Parameters of Accreting T Tauri Stars with Observationally Derived Magnetic Maps

Star	Spec. Type	T_{eff} (K) ^b	$\log(L_*/L_\odot)$ ^b	P_{rot} (days)	τ_c (days)	Binary?	Separation (AU)	Reference
Stars with strong dipole components and dominantly axisymmetric large-scale magnetic fields								
AA Tau	K7	4000 ± 100	0.0 ± 0.1	8.22	230	no	...	1
BP Tau	K7	4055 ± 112	-0.03 ± 0.1	7.6	237	no	...	2
Stars with dominant high-order magnetic field components ($\ell > 1$) and axisymmetric large-scale magnetic fields								
V2129 Oph ^c	K5	4500 ± 100	0.15 ± 0.1	6.53	182	yes	78	3,4
GQ Lup	K7	4300 ± 50	0.0 ± 0.1	8.4	199	yes	100	5
TW Hya	K7	4075 ± 75	-0.46 ± 0.1	3.56	180	no	...	6
MT Ori	K2	4600 ± 100	1.49 ± 0.13	8.53	322	no	...	7
Stars with complex non-axisymmetric large-scale magnetic fields and weak dipole components								
V4046 Sgr A	K5	4370 ± 100	-0.39 ± 0.1	2.42	117	yes	0.041	8
V4046 Sgr B	K5	4100 ± 100	-0.57 ± 0.1	2.42	130	yes	0.041	8
CR Cha	K2	4900 ± 100	0.58 ± 0.13	2.3	92	no	...	9
CV Cha	G8	5500 ± 100	0.89 ± 0.08	4.4	56	yes	1596	9
V2247 Oph ^d	M1	3500 ± 150	-0.33 ± 0.1	3.5	222	yes	36	10

Notes.

^a Columns 1-2: star name and observation date; Columns 3-6: effective temperature, luminosity, rotation period, and an estimate of the local convective turnover time discussed in Section 5.2; Columns 7-8: binary star status and separation; Column 9: reference where effective temperature and luminosity assignment is discussed.

^b Error estimates are discussed in Section 2, fifth and sixth paragraphs.

^c The V2129 Oph luminosity was updated from that used in Donati et al. (2007) by Donati et al. (2011a) using a more refined distance estimate to the ρ -Oph star-forming region of 120 pc (Loinard et al. 2008).

^d The luminosity of V2247 Oph has been updated from Donati et al. (2010a) using the Loinard et al. (2008) distance estimate.

References. (1) Donati et al. 2010b; (2) Donati et al. 2008a; (3) Donati et al. 2007; (4) Donati et al. 2011a; (5) Donati et al. 2012; (6) Donati et al. 2011b; (7) Skelly et al. 2012; (8) Donati et al. 2011c; (9) Hussain et al. 2009; (10) Donati et al. 2010a.

increasing the field complexity. The binary magnetospheric structure is highly complex and will be presented in a future paper. A circular polarization signal was not detected in the accretion-related emission lines, consistent with the complex magnetic geometries and likely indicative of accretion spots being distributed across many opposite polarity regions (Donati et al. 2011c). The binary orbit is circularized and synchronized with accretion occurring from a circumbinary disk (Stempels & Gahm 2004; Rodriguez et al. 2010). Recent numerical simulations suggest that small local circumstellar disks, distinct from the global circumbinary disk, may also form around the individual stars (de Val-Borro et al. 2011). As with TW Hya (see Appendix A.2.3), V4046 Sgr (age ~ 13 Myr) is still accreting at an age when most T Tauri stars have lost their disks (e.g., Fedele et al. 2010). The masses of V4046 Sgr AB listed in Table 2 are derived from the PMS evolution models and placing the stars on the H-R diagram. These can be compared to the more accurate dynamical masses of $0.912 M_\odot$ and $0.873 M_\odot$ calculated by Stempels & Gahm (2004) for V4046 Sgr A and V4046 Sgr B, respectively. Both binary components have ended the fully convective phase of evolution with the primary and secondary have core masses of roughly 50% and 40% of their respective stellar masses using the models of Siess et al. (2000).

A.3.2. CR Cha

CR Cha hosts a particularly complex magnetic field with a significant fraction of the magnetic energy in high ℓ -number field modes (Hussain et al. 2009). Unlike the other T Tauri stars discussed in this paper, CR Cha (and CV Cha, see below) was observed with SemelPol, a spectropolarimeter at the Anglo-Australian Telescope. As with V4046 Sgr, a circular polarization signal was not detected in the accretion-related emission lines.

Hussain et al. (2009) noted that this non-detection may have been due to insufficient S/N. CR Cha is too far south to be re-observed with ESPaDOnS. However, as Stokes V signals were not detected in the emission lines in the higher S/N ESPaDOnS spectra of V4046 Sgr, and as the magnetic maps of V4046 Sgr AB and CR Cha reveal a similar level of field complexity, a more likely explanation is that magnetospheric accretion onto the surface of CR Cha occurs into several distributed opposite polarity magnetic regions, yielding a net polarization signal of zero due to the flux cancellation effect. Because of this the value listed for the dipole component of the multipolar field of CR Cha in Table 2 is a lower limit and the true value may be larger. According to the Siess et al. (2000) models it has a substantial radiative core $M_{\text{core}}/M_* = 0.65$.

A.3.3. CV Cha

The magnetic field of CV Cha is highly complex with many high-order field components (Hussain et al. 2009). As with CR Cha a circular polarization signal was not detected in the accretion-related emission lines, and the dipole component listed in Table 2 is likely a lower limit to the true value. CV Cha is the primary star of a large separation (1596 AU) binary system; CW Cha being the secondary star (Reipurth & Zinnecker 1993). Of the two Chamealeon I stars for which magnetic maps have been published, CV Cha has the larger mass accretion rate, $\log \dot{M} = -7.5 M_\odot \text{ yr}^{-1}$ compared to $\log \dot{M} = -9.0 M_\odot \text{ yr}^{-1}$ for CR Cha (Hussain et al. 2009). CV Cha is the earliest spectral-type star in our sample (see Table 1), is well into the Henyey phase of its evolution, and is almost entirely radiative ($M_{\text{core}}/M_* \approx 1.0$; Siess et al. 2000).

Table 2
Parameters of Accreting T Tauri Stars with Observationally Derived Magnetic Maps

Star	Date	Siess et al. (2000)			Tognelli et al. (2011)			B_{dip} (kG) ^b	Reference
		M_*/M_{\odot}	M_{core}/M_*	Age (Myr)	M_*/M_{\odot}	M_{core}/M_*	Age (Myr)		
Stars with strong dipole components and dominantly axisymmetric large-scale magnetic fields									
AA Tau	2007 Dec	0.70	0.00	1.42	0.63	0.00	1.39	1.9	1
...	2009 Jan	1.7	1
BP Tau ^c	2006 Feb	0.75	0.00	1.80	0.69	0.00	1.64	1.2	2
...	2006 Dec	1.0	2
Stars with dominant high-order magnetic field components ($\ell > 1$) and axisymmetric large-scale magnetic fields									
V2129 Oph ^d	2005 Jun	1.36	0.19	3.67	1.14	0.10	2.28	0.3	3,4
...	2009 Jul	1.0	4
GQ Lup	2009 Jul	1.06	0.13	3.33	0.93	0.02	2.39	1.1	5
...	2011 Jun	0.9	5
TW Hya	2008 Mar	0.83	0.18	9.17	0.84	0.27	7.13	0.4	6
...	2010 Mar	0.7	6
MT Ori	2008 Dec	2.7	>0.03, <0.36	0.24	1.96	0.00	0.18	<0.1	7
Stars with complex non-axisymmetric large-scale magnetic fields and weak dipole components									
V4046 Sgr A	2009 Sep	0.91	0.47	13.0	0.98	0.64	12.0	0.1	8
V4046 Sgr B	2009 Sep	0.87	0.40	13.0	0.85	0.50	12.1	0.08	8
CR Cha	2006 Apr	1.96	0.65	2.89	1.78	0.39	1.67	>0.09	9
CV Cha	2006 Apr	2.04	0.98	4.51	2.19	0.94	2.97	>0.02	9
V2247 Oph ^e	2008 Jul	0.36	0.00	1.4	0.35	0.00	1.67	0.1	10

Notes.

^a Columns 3-5: stellar mass, radiative core mass relative to the stellar mass, and the age derived from the models of Siess et al. (2000); Columns 6-8: as Columns 3-5 but from the models of Tognelli et al. (2011). Column 9: rotation period; Columns 10-11: the polar strength of the dipole B_{dip} field component with reference.

^b All of the stars host multipolar magnetic fields, but we list only the dipole component given its importance to the star-disk interaction. The large-scale magnetic fields of AA Tau, BP Tau, V2129 Oph, and TW Hya are well described by a tilted dipole plus a tilted octupole field component (Gregory & Donati 2011), as is the field of GQ Lup (Donati et al. 2012).

^c The magnetic parameters for BP Tau are based on an old version of the magnetic imaging code and will be updated in a forthcoming paper, see Appendix A.1.2.

^d The 2005 Jun V2129 Oph data presented in Donati et al. (2007) were reanalyzed by Donati et al. (2011a).

^e Parameters for V2247 Oph updated from Donati et al. (2010a).

References. (1) Donati et al. 2010b; (2) Donati et al. 2008a; (3) Donati et al. 2007; (4) Donati et al. 2011a; (5) Donati et al. 2012; (6) Donati et al. 2011b; (7) Skelly et al. 2012; (8) Donati et al. 2011c; (9) Hussain et al. 2009; (10) Donati et al. 2010a.

A.3.4. V2247 Oph

V2247 Oph is the lowest mass T Tauri star for which magnetic maps have been published. It is fully convective and it is found to host a complex magnetic field with a weak dipole component (Donati et al. 2010a). Its topology is therefore similar to the more massive T Tauri stars which have developed substantial radiative cores, rather than the simple fields of the other fully convective stars AA Tau and BP Tau. Its mass of $\sim 0.36 M_{\odot}$ has been obtained from the Siess et al. (2000) models using a luminosity appropriate for a distance to the ρ Oph star-forming region of 120 pc (Loinard et al. 2008). V2247 Oph is weakly accreting and has previously been classified as a non-accreting weak-line T Tauri star (e.g., Bouvier & Appenzeller 1992). However, all of the accretion-related emission lines are present in the ESPaDOnS spectra, with evidence for a weak accretion rate. The accretion rate is found to be highly variable over timescales of order a week (Donati et al. 2010a), and over several years (Littlefair et al. 2004), reaching peaks of around $\log \dot{M} \approx -9 M_{\odot} \text{ yr}^{-1}$. The spectral energy distribution of V2247 Oph suggests that its disk is rather evolved with a large inner (dust) disk gap (Gras-Velázquez & Ray 2005). This may be due to a nearby binary companion star (Simon et al. 1987), separated by 36 AU adopting the distance given

above, suggesting that accretion occurs from a circumbinary disk. V2247 Oph is rotating about twice as fast ($P_{\text{rot}} \sim 3.5$ days) as the other fully convective stars in the sample, AA Tau ($P_{\text{rot}} = 8.22$ days) and BP Tau ($P_{\text{rot}} = 7.6$ days). As speculated by Donati et al. (2010a) the faster spin rate of V2247 Oph may be a direct reflection of its complex magnetic field. Stars with magnetic fields with weaker dipole components would have disks that are magnetospherically truncated closer to the star, potentially resulting in a larger spin-up torque in comparison to that experienced by stars with stronger dipole components that are able to truncate their disks at larger radii (e.g., Matt & Pudritz 2005). The variation in field topology between the more massive fully convective PMS stars and the low-mass PMS star V2247 Oph is similar to what has been found for the MS M-dwarfs, see Section 3.3 and Morin et al. (2010, 2011).

APPENDIX B

THE FULLY CONVECTIVE LIMIT AS A FUNCTION OF STELLAR AGE

The age at which a star ends the fully convective phase of evolution (the fully convective limit) is a function of stellar mass (see Figure 8). From the Siess et al. (2000) models ($Z = 0.02$

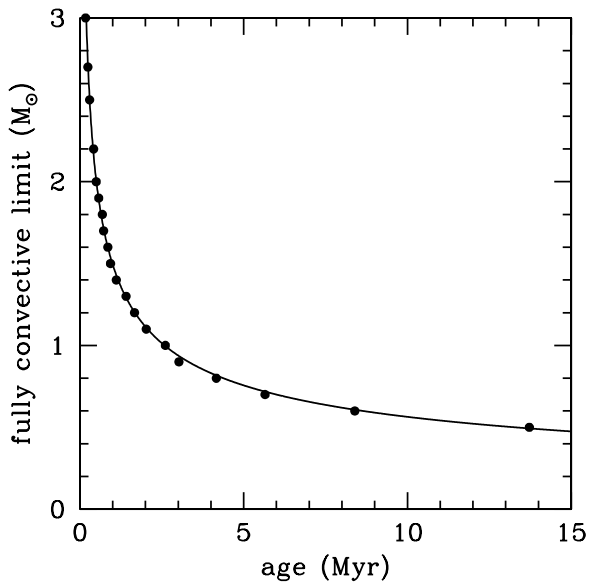


Figure 8. Fully convective limit as a function of age. A power-law fit (solid line) to the data from the Siess et al. (2000) models (points) is given by Equation (B1). At a given age stars of higher mass than the fully convective limit have developed radiative cores while those of lower mass remain fully convective.

with convective overshooting) we can estimate the age at which the fully convective phase ends,

$$\text{age [Myr]} \approx \left(\frac{1.494}{M_*/M_\odot} \right)^{2.364}, \quad (\text{B1})$$

which is the power-law fit, the solid black line in Figure 8 (stars below $\sim 0.35 M_\odot$ remain fully convective, e.g., Chabrier & Baraffe 1997). Thus, a $0.5 M_\odot$ star ends the fully convective phase and develops a radiative core at an age of ~ 13.3 Myr, while a $1 M_\odot$ and a $2 M_\odot$ star develop a radiative core at an age of ~ 2.6 Myr and ~ 0.5 Myr, respectively. The early development of a radiative core, and its more rapid growth, for more massive

stars leads to a gap in the observed color–magnitude diagrams of young PMS clusters. The size of which, as discussed by Mayne et al. (2007), is a function of age and can possibly be used as a distance-independent age indicator.

Recently, new mass tracks and isochrones have been published by Tognelli et al. (2011): the Pisa PMS stellar evolution models. The Pisa model equivalent of Equation (B1) is

$$\text{age [Myr]} \approx \left(\frac{1.448}{M_*/M_\odot} \right)^{2.101}, \quad (\text{B2})$$

where $Z = 0.02$, $Y = 0.288$, $\alpha = 1.68$, and $X_D = 2 \times 10^{-5}$ have been assumed. Thus, in the Pisa models a $0.5 M_\odot$ star ends the fully convective phase and develops a radiative core at an age of ~ 9.3 Myr, while a $1 M_\odot$ and a $2 M_\odot$ star develop a radiative core at an age of ~ 2.2 Myr and ~ 0.5 Myr, respectively. A comparison between Equations (B1) and (B2) reveals that the fully convective phase ends at approximately the same age for high-mass T Tauri stars, with differences of < 0.5 Myr for stars of mass $> 0.95 M_\odot$, but this difference is larger for lower mass stars and exceeds 4 Myr for stars of mass $< 0.5 M_\odot$. As lower mass stars are more likely to lose their disk before a radiative core develops, and therefore before any drastic change in the large-scale field topology occurs, then the difference in the age at which a core develops between the Siess et al. (2000) and the Tognelli et al. (2011) models is not too significant. For example, for a $0.5 M_\odot$ star the fully convective phase ends at 13.3 Myr or 9.3 Myr in the Siess et al. (2000) and Tognelli et al. (2011) models, respectively. However, the fraction of stars with disks (substantial, primordial, dusty disks) is only $\sim 0.5\%$ or $\sim 2.4\%$ at such ages, using the disk lifetime estimate given by Mamajek (2009). Thus, the 4 Myr year difference in age between the end of the fully convective phase in the two PMS evolution models has little effect in terms of any stellar spin-up that may occur when a star is still coupled to its disk when a radiative core develops. Of course, we must also account for the fact that for a given star the different mass tracks and isochrones of each model yield different age and mass estimates.

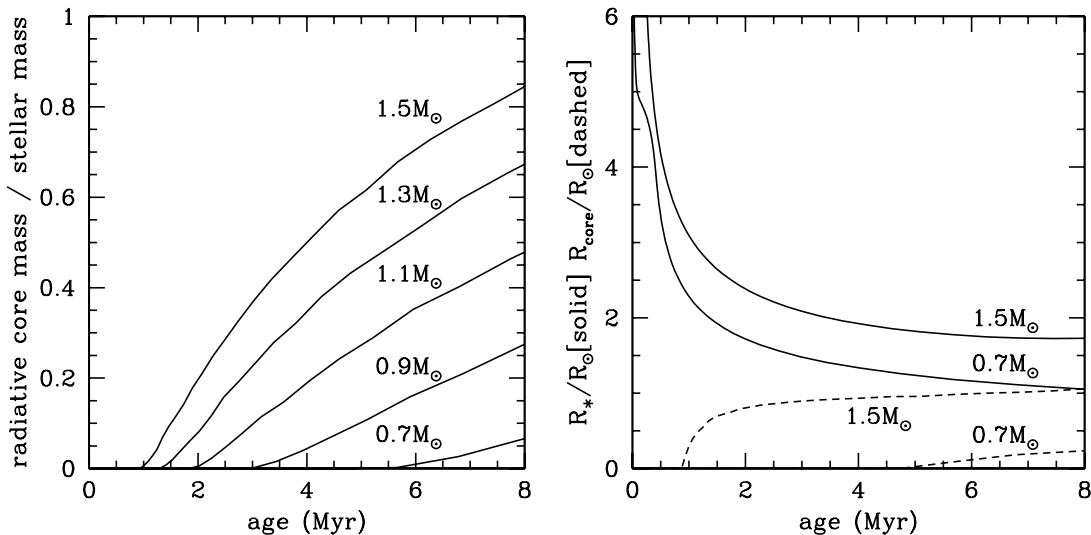


Figure 9. Left: the growth of the radiative core mass relative to the stellar mass as a function of age obtained from the Siess et al. (2000) PMS stellar evolution models for stars of different mass. An ordinate value of zero (one) represents a star which has a fully convective (completely radiative) interior. Higher mass T Tauri stars develop radiative cores at a younger age, and the mass of the core relative to the stellar mass increases faster, compared to lower mass T Tauri stars. Right: the decrease in the stellar radius (R_* ; solid lines) and increase in the core radius (R_{core} ; dashed lines) with age. Only stellar radii below $6 R_\odot$, and the behavior for a $1.5 M_\odot$ star and a $0.7 M_\odot$ star, are shown for clarity. The brief slowing of the contraction for the $0.7 M_\odot$ star at ~ 0.5 Myr is caused by deuterium burning; this occurs at an earlier age and off the vertical scale for the $1.5 M_\odot$ star.

REFERENCES

- Adams, F. C., & Gregory, S. G. 2012, *ApJ*, **744**, 55
- Akeson, R. 2008, *New Astron. Rev.*, **52**, 94
- Akeson, R. L., Walker, C. H., Wood, K., et al. 2005, *ApJ*, **622**, 440
- Alexander, F., & Preibisch, T. 2012, *A&A*, **539**, A64
- Argiroffi, C., Flaccomio, E., Bouvier, J., et al. 2011, *A&A*, **530**, A1
- Argiroffi, C., Maggio, A., Montmerle, T., et al. 2012, *ApJ*, **752**, 100
- Aurière, M. 2003, Proc. Magnetism and Activity of the Sun and Stars, EAS Publications Series, 9, ed. J. Arnaud & N. Meunier (Les Ulis, France: EDP Sciences), 105
- Baraffe, I., & Chabrier, G. 2010, *A&A*, **521**, A44
- Bouvier, J., & Appenzeller, I. 1992, *A&AS*, **92**, 481
- Bouvier, J., Cabrit, S., Fernandez, M., Martin, E. L., & Mathews, J. M. 1993, *A&A*, **272**, 176
- Brown, S. F., Donati, J.-F., Rees, D. E., & Semel, M. 1991, *A&A*, **250**, 463
- Browning, M. K. 2008, *ApJ*, **676**, 1262
- Calvet, N., & Gullbring, E. 1998, *ApJ*, **509**, 802
- Calvet, N., Muzerolle, J., Briceño, C., et al. 2004, *AJ*, **128**, 1294
- Carpenter, J. M., Mamajek, E. E., Hillenbrand, L. A., & Meyer, M. R. 2006, *ApJ*, **651**, L49
- Chabrier, G., & Baraffe, I. 1997, *A&A*, **327**, 1039
- Chuntonov, G. A., Smirnov, D. A., & Lamzin, S. A. 2007, *Astron. Lett.*, **33**, 38
- Cieza, L. A., Schreiber, M. R., Romero, G. A., et al. 2010, *ApJ*, **712**, 925
- Currie, T., & Kenyon, S. J. 2009, *AJ*, **138**, 703
- D'Antona, F., Ventura, P., & Mazzitelli, I. 2000, *ApJ*, **543**, L77
- de Val-Borro, M., Gahm, G. F., Stempels, H. C., & Pepliński, A. 2011, *MNRAS*, **413**, 2679
- Donati, J.-F. 2001, Astromotography, Indirect Imaging Methods in Observational Astronomy, Lecture Notes in Physics, Vol. 573, ed. H. M. J. Boffin, D. Steeghs, & J. Cuypers (Berlin: Springer)
- Donati, J.-F. 2003, in ASP Conf. Ser. 307, Solar Polarization, ed. J. Trujillo-Bueno & J. S. Almeida (San Francisco, CA: ASP), 41
- Donati, J.-F. 2011, in IAU Symp. 271, Astrophysical Dynamics: From Stars to Galaxies, ed. N. Brummell, A. S. Brun, M. S. Miesch, & Y. Ponty (Cambridge: Cambridge Univ. Press), 23
- Donati, J.-F., Bouvier, J., Walter, F. M., et al. 2011a, *MNRAS*, **412**, 2454
- Donati, J.-F., & Brown, S. F. 1997, *A&A*, **326**, 1135
- Donati, J.-F., Collier Cameron, A., Semel, M., et al. 2003, *MNRAS*, **345**, 1145
- Donati, J.-F., Gregory, S. G., Alencar, S. H. P., et al. 2011b, *MNRAS*, **417**, 472
- Donati, J.-F., Gregory, S. G., Alencar, S. H. P., et al. 2012, *MNRAS* [astro-ph/1206.1770], in press
- Donati, J.-F., Gregory, S. G., Montmerle, T., et al. 2011c, *MNRAS*, **417**, 1747
- Donati, J.-F., Howarth, I. D., Jardine, M. M., et al. 2006, *MNRAS*, **370**, 629
- Donati, J.-F., Jardine, M. M., Gregory, S. G., et al. 2007, *MNRAS*, **380**, 1297
- Donati, J.-F., Jardine, M. M., Gregory, S. G., et al. 2008a, *MNRAS*, **386**, 1234
- Donati, J.-F., & Landstreet, J. D. 2009, *ARA&A*, **47**, 333
- Donati, J.-F., Morin, J., Petit, P., et al. 2008b, *MNRAS*, **390**, 545
- Donati, J.-F., Semel, M., Carter, B. D., Rees, D. E., & Collier Cameron, A. 1997, *MNRAS*, **291**, 658
- Donati, J.-F., Skelly, M. B., Bouvier, J., et al. 2010a, *MNRAS*, **402**, 1426
- Donati, J.-F., Skelly, M. B., Bouvier, J., et al. 2010b, *MNRAS*, **409**, 1347
- Dunstone, N. J., Hussain, G. A. J., Collier Cameron, A., et al. 2008a, *MNRAS*, **387**, 481
- Dunstone, N. J., Hussain, G. A. J., Collier Cameron, A., et al. 2008b, *MNRAS*, **387**, 1525
- Eisner, J. A., Graham, J. R., Akeson, R. L., & Najita, J. 2009, *ApJ*, **692**, 309
- Eisner, J. A., Monnier, J. D., Woillez, J., et al. 2010, *ApJ*, **718**, 774
- Endal, A. S., & Sofia, S. 1981, *ApJ*, **243**, 625
- Ercolano, B., Bastian, N., Spezzi, L., & Owen, J. 2011, *MNRAS*, **416**, 439
- Fedele, D., van den Ancker, M. E., Henning, T., Jayawardhana, R., & Oliveira, J. M. 2010, *A&A*, **510**, A72
- Getman, K. V., Broos, P. S., Salter, D. M., Garmire, G. P., & Hogerheijde, M. R. 2011, *ApJ*, **730**, 6
- Ghez, A. M., Neugebauer, G., & Matthews, K. 1993, *AJ*, **106**, 2005
- Gilliland, R. L. 1986, *ApJ*, **300**, 339
- Gorti, U., Dullemond, C. P., & Hollenbach, D. 2009, *ApJ*, **705**, 1237
- Goudard, L., & Dormy, E. 2008, *Europhys. Lett.*, **835**, 59001
- Gras-Velázquez, À., & Ray, T. P. 2005, *A&A*, **443**, 541
- Gregory, S. G., & Donati, J.-F. 2011, *Astron. Nachr.*, **332**, 1027
- Gregory, S. G., Jardine, M., Collier Cameron, A., & Donati, J.-F. 2005, in 13th Cambridge Workshop on Cool Stars, Stellar Systems and the Sun, ed. F. Favata, G. A. J. Hussain, & B. Battrick (ESA SP-560; Noordwijk: ESA), 191
- Gregory, S. G., Jardine, M., Gray, C. G., & Donati, J.-F. 2010, *Rep. Prog. Phys.*, **73**, 126901
- Gregory, S. G., Jardine, M., Simpson, I., & Donati, J.-F. 2006, *MNRAS*, **371**, 999
- Gregory, S. G., Matt, S. P., Donati, J.-F., & Jardine, M. 2008, *MNRAS*, **389**, 1839
- Gullbring, E., Hartmann, L., Briceno, C., & Calvet, N. 1998, *ApJ*, **492**, 323
- Hartmann, L. 2001, *AJ*, **121**, 1030
- Hartmann, L. (ed.) 2009, *Accretion Processes in Star Formation* (2nd ed.; Cambridge: Cambridge Univ. Press)
- Hartmann, L., Calvet, N., Gullbring, E., & D'Alessio, P. 1998, *ApJ*, **495**, 385
- Hayashi, C. 1961, *PASJ*, **13**, 450
- Heney, L., Vardya, M. S., & Bodenheimer, P. 1965, *ApJ*, **142**, 841
- Hillenbrand, L. A., Bauermeister, A., & White, R. J. 2008, in ASP Conf. Ser. 384, 14th Cambridge Workshop on Cool Stars, Stellar Systems, and the Sun, ed. G. van Belle (San Francisco, CA: ASP), 200
- Hillenbrand, L. A., & White, R. J. 2004, *ApJ*, **604**, 741
- Hussain, G. A. J. 2012, *Astron. Nachr.*, **333**, 4
- Hussain, G. A. J., Collier Cameron, A., Jardine, M. M., et al. 2009, *MNRAS*, **398**, 189
- Hussain, G. A. J., Jardine, M., Donati, J.-F., et al. 2007, *MNRAS*, **377**, 1488
- Isella, A., Tatulli, E., Natta, A., & Testi, L. 2008, *A&A*, **483**, L13
- Johns-Krull, C. M. 2007, *ApJ*, **664**, 975
- Johns-Krull, C. M., Valenti, J. A., Hatzes, A. P., & Kanaan, A. 1999a, *ApJ*, **510**, L41
- Johns-Krull, C. M., Valenti, J. A., & Koresko, C. 1999b, *ApJ*, **516**, 900
- Johns-Krull, C. M., Valenti, J. A., & Linsky, J. L. 2000, *ApJ*, **539**, 815
- Jung, Y. K., & Kim, Y.-C. 2007, *J. Astron. Space Sci.*, **24**, 1
- Kastner, J. H., Huenemoerder, D. P., Schulz, N. S., Canizares, C. R., & Weintraub, D. A. 2002, *ApJ*, **567**, 434
- Kim, Y.-C., & Demarque, P. 1996, *ApJ*, **457**, 340
- Königl, A. 1991, *ApJ*, **370**, L39
- Kraus, S., Preibisch, T., & Ohnaka, K. 2008, *ApJ*, **676**, 490
- Landin, N. R., Mendes, L. T. S., & Vaz, L. P. R. 2010, *A&A*, **510**, A46
- Lavigne, J.-F., Doyon, R., Lafrenière, D., Marois, C., & Barman, T. 2009, *ApJ*, **704**, 1098
- Lejeune, T., & Schaerer, D. 2001, *A&A*, **366**, 538
- Littlefair, S. P., Naylor, T., Harries, T. J., Retter, A., & O'Toole, S. 2004, *MNRAS*, **347**, 937
- Loinard, L., Torres, R. M., Mioduszewski, A. J., & Rodríguez, L. F. 2008, *ApJ*, **675**, L29
- Long, M., Romanova, M. M., Kulkarni, A. K., & Donati, J.-F. 2011, *MNRAS*, **413**, 1061
- Long, M., Romanova, M. M., & Lamb, F. K. 2012, *New Astron.*, **17**, 232
- Long, M., Romanova, M. M., & Lovelace, R. V. E. 2007, *MNRAS*, **374**, 436
- Long, M., Romanova, M. M., & Lovelace, R. V. E. 2008, *MNRAS*, **386**, 1274
- Luhman, K. L., Allen, L. E., Allen, P. R., et al. 2008, *ApJ*, **675**, 1375
- Mamajek, E. E. 2009, in AIP Conf. Proc. 1158, Exoplanets and Disks: Their Formation and Diversity, ed. T. Usuda, M. Ishii, & M. Tamura (Melville, NY: AIP), 3
- Marsden, S. C., Jardine, M. M., Ramírez Vélez, J. C., et al. 2011, *MNRAS*, **413**, 1922
- Matt, S., & Pudritz, R. E. 2005, *MNRAS*, **356**, 167
- Matt, S. P., Pinzón, G., de la Reza, R., & Greene, T. P. 2010, *ApJ*, **714**, 989
- Matt, S. P., Pinzón, G., Greene, T. P., & Pudritz, R. E. 2012, *ApJ*, **745**, 101
- Mayne, N. J. 2010, *MNRAS*, **408**, 1409
- Mayne, N. J., & Naylor, T. 2008, *MNRAS*, **386**, 261
- Mayne, N. J., Naylor, T., Littlefair, S. P., Saunders, E. S., & Jeffries, R. D. 2007, *MNRAS*, **375**, 1220
- Millan-Gabet, R., Malbet, F., Akeson, R., et al. 2007, in Protostars and Planets V, ed. B. Reipurth, D. Jewitt, & K. Keil (Tucson, AZ: Univ. Arizona Press), 539
- Mohanty, S., & Shu, F. H. 2008, *ApJ*, **687**, 1323
- Morin, J., Donati, J.-F., Petit, P., et al. 2008, *MNRAS*, **390**, 567
- Morin, J., Donati, J.-F., Petit, P., et al. 2010, *MNRAS*, **407**, 2269
- Morin, J., Donati, J.-F., Petit, P., et al. 2011, in IAU Symp. 273, The Physics of Sun and Star Spots, ed. D. P. Choudhary & K. G. Strassmeier (Cambridge: Cambridge Univ. Press), 181
- Morin, J., Dormy, E., Schrunner, M., & Donati, J.-F. 2011, *MNRAS*, **418**, 133
- Najita, J., Carr, J. S., & Mathieu, R. D. 2003, *ApJ*, **589**, 931
- Neuhäuser, R., Guenther, E. W., Wuchterl, G., et al. 2005, *A&A*, **435**, L13
- Palla, F. 2001, in ASP Conf. Proc. 243, From Darkness to Light: Origin and Evolution of Young Stellar Clusters, ed. T. Montmerle & P. André (San Francisco, CA: ASP), 525
- Palla, F., Randich, S., Flaccomio, E., & Pallavicini, R. 2005, *ApJ*, **626**, L49
- Palla, F., & Stahler, S. W. 2001, *ApJ*, **553**, 299
- Pinsonneault, M. 1997, *ARA&A*, **35**, 557
- Pizzolato, N., Maggio, A., Micela, G., Sciortino, S., & Ventura, P. 2003, *A&A*, **397**, 147

- Preibisch, T., Kim, Y.-C., Favata, F., et al. 2005, *ApJS*, **160**, 401
- Qi, C., Ho, P. T. P., Wilner, D. J., et al. 2004, *ApJ*, **616**, L11
- Ragland, S., Akeson, R. L., Armandroff, T., et al. 2009, *ApJ*, **703**, 22
- Rebull, L. M., Stauffer, J. R., Ramirez, S. V., et al. 2006, *AJ*, **131**, 2934
- Reiners, A., & Basri, G. 2009, *A&A*, **496**, 787
- Reipurth, B., & Zinnecker, H. 1993, *A&A*, **278**, 81
- Roberts, P. H. 1988, *Geophys. Astrophys. Fluid Dyn.*, **44**, 3
- Rodriguez, D. R., Kastner, J. H., Wilner, D., & Qi, C. 2010, *ApJ*, **720**, 1684
- Romanova, M. M., Long, M., Lamb, F. K., Kulkarni, A. K., & Donati, J.-F. 2011, *MNRAS*, **411**, 915
- Romanova, M. M., Ustyugova, G. V., Koldoba, A. V., & Lovelace, R. V. E. 2004a, *ApJ*, **610**, 920
- Romanova, M. M., Ustyugova, G. V., Koldoba, A. V., & Lovelace, R. V. E. 2004b, *ApJ*, **616**, 151
- Salter, D. M., Kóspál, Á., Getman, K. V., et al. 2010, *A&A*, **521**, A32
- Saunders, E. S., Naylor, T., Mayne, N., & Littlefair, S. P. 2009, *MNRAS*, **397**, 405
- Schrinner, M., Petitdemange, L., & Dormy, E. 2012, *ApJ*, **752**, 121
- Sicilia-Aguilar, A., Hartmann, L. W., Briceño, C., Muzerolle, J., & Calvet, N. 2004, *AJ*, **128**, 805
- Siess, L. 2001, in ASP Conf. Proc. 243, From Darkness to Light: Origin and Evolution of Young Stellar Clusters, ed. T. Montmerle & P. André (San Francisco, CA: ASP), 581
- Siess, L., Dufour, E., & Forestini, M. 2000, *A&A*, **358**, 593
- Simon, M., Dutrey, A., & Guilloteau, S. 2000, *ApJ*, **545**, 1034
- Simon, M., Howell, R. R., Longmore, A. J., et al. 1987, *ApJ*, **320**, 344
- Skelly, M. B., Donati, J.-F., Bouvier, J., et al. 2010, *MNRAS*, **403**, 159
- Skelly, M. B., Donati, J.-F., Bouvier, J., et al. 2012, *MNRAS*, submitted
- Soderblom, D. R. 2010, *ARA&A*, **48**, 581
- Stempels, H. C., & Gahm, G. F. 2004, *A&A*, **421**, 1159
- Symington, N. H., Harries, T. J., Kurosawa, R., & Naylor, T. 2005, *MNRAS*, **358**, 977
- Tognelli, E., Prada Moroni, P. G., & Degl'Innocenti, S. 2011, *A&A*, **533**, A109
- Valenti, J. A., & Johns-Krull, C. M. 2004, *Ap&SS*, **292**, 619
- Waite, I. A., Marsden, S. C., Carter, B. D., et al. 2011, *MNRAS*, **413**, 1949
- Ward-Thompson, D., & Whitworth, A. P. (ed.) 2011, *An Introduction to Star Formation* (Cambridge: Cambridge Univ. Press)
- Williams, J. P., & Cieza, L. A. 2011, *ARA&A*, **49**, 67
- Willis, D. M., & Osborne, A. D. 1982, *Geophys. J. Int.*, **68**, 765
- Yang, H., & Johns-Krull, C. M. 2011, *ApJ*, **729**, 83